

Chapter 5

Cast Iron–Based Alloys



Dawid Myszka

Abbreviations and Symbols

<i>CI</i>	Cast iron
<i>DI</i>	Ductile iron
<i>ADI</i>	Austempered ductile iron
<i>ADI_{xxx}_{xxx}</i> (for example: <i>EADI₄₀₀₃₀</i>)	Determination of isothermal transformation parameters of austempered ductile iron (in the example: $T_{it} = 400\text{ °C}$, $t_{it} = 30\text{ min.}$)
<i>CADI</i>	Carbide austempered ductile iron
<i>DADI</i>	Direct austempered ductile iron
<i>Q&T</i>	Quenched and tempered
<i>HT</i>	Heat treated
<i>EN-GJL</i>	Gray iron grades according to European Standard EN 1561
<i>C_E</i>	Carbon equivalent
<i>Gr</i>	Graphite
<i>P</i>	Pearlite
α , <i>F</i>	Ferrite
δ	High-temperature ferrite
γ , <i>A</i> ,	Austenite
γ^0	Primary austenite
γ_{HC}	High-carbon austenite
α' , <i>M</i>	Martensite
$\alpha + \gamma_{HC}$, <i>AF</i>	Ausferrite

D. Myszka (✉)

Department of Metal Forming and Foundry Engineering, Warsaw University of Technology, Warszawa, Mazowsze, Poland

B_U	Upper bainite
B_L	Lower bainite
B_S, B_F	Start and end of bainitic transformation,
A_S, A_F	Start and end of ausferritic transformation
M_S, M_F	Temperature of the beginning and end of marten- sitic transformation [$^{\circ}\text{C}$]
$T_{\gamma,A}$	Austenitizing temperature [$^{\circ}\text{C}$]
$t_{\gamma,A}$	Austenitizing time [min.]
T_{it}	Isothermal transformation temperature [$^{\circ}\text{C}$]
t_{it}	Isothermal transformation time [min.]
T_0	Temperatura pokojowa [$^{\circ}\text{C}$]
C_{γ}^A	Carbon content in austenite at austenitizing temper- ature [%]
C_{γ}	Carbon content in austenite [%]
X_{γ}	Austenite content in the ausferritic mixture [%]
R_{YS}	Yield strength [MPa]
R_{TS}	Tensile strength [MPa]
K_{IC}	Fracture toughness [$\text{MPa} \times \text{m}^{1/2}$]
D	Critical diameter [mm]
$TRIP$	Transformation-induced plasticity
SEM	Scanning electron microscope
TEM	Transmission electron microscope
LM	Light microscope
XRD	X-ray diffraction

5.1 Cast Iron Vs. Steel

Among all foundry alloys for structural applications, cast iron is the best known and most frequently used material (Fig. 5.1) [1–13]. As an iron-carbon alloy, it is often confused with or compared to steel. And yet, as we shall see in this chapter, its features are completely different from steels. To discover this, cast iron needs to be studied more carefully.

5.1.1 Basics of Cast Iron

The great popularity of cast iron in both industry and research areas has survived to this day despite the fact that this casting material has been known since 1000 BC [14]. The devices for cast iron melting, i.e., shaft furnaces in China and bloomeries first, blast furnaces in Europe next, and, finally, cupolas are milestones in the development of civilization.

In addition to the practical experience of artists, i.e., foundry men, the gradual entering of science into the field of cast iron production enabled further discoveries

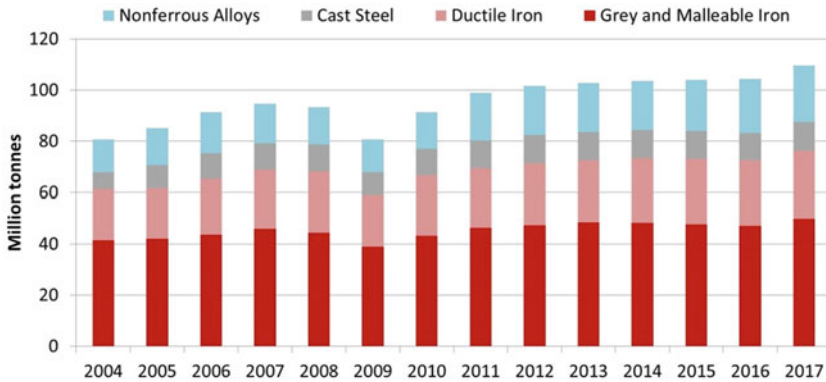


Fig. 5.1 Trends in world casting production in the years 2004–2017. (Author’s own analysis based on [1–13])

that led to unflagging interest in this material lasting to the present day. It is enough to mention A.F. Meehan who in 1922 developed a method for the manufacture of inoculated cast iron, or H. Morrogh and A.P. Gagnebin who in 1947 invented the cast iron with nodular graphite known also as ductile iron. Those were the turning points in the use of cast iron as a construction material but by no means the end of spectacular discoveries in this field. Heat treatment, and especially the austempering treatment of ductile iron, developed at the end of the twentieth century as well as a multitude of scientific publications that have appeared in recent years best prove the fact that studies of this material are going on all the time [15, 16].

According to the most general definition, cast iron is an iron-carbon alloy, usually with the carbon content ranging from 2 to 4 wt.%. Typically, cast iron also contains other elements. It is produced by remelting pig iron, cast iron scrap, and steel scrap and solidifies with eutectic transformation. It contrasts with cast steel which, being also an iron-carbon alloy with other elements, has no eutectic in its composition. Depending on whether the cast iron solidifies in a stable or metastable system (Fig. 5.2), graphite eutectic or cementite eutectic (ledeburite) will form, respectively. Depending on the form of carbon, bonded or free (graphite), the cast iron is said to be white or gray, respectively (Fig. 5.2). The adjective *white* or *gray* in the name of the cast iron reflects the color of the fracture, which is bright with metallic shimmer in white cast iron and gray in gray cast iron. The gray color in the latter case is associated with the presence of graphite in the fracture.

The most spectacular properties of cast iron are obtained primarily in ductile iron, the invention of which eliminated the fundamental disadvantage of this material, i.e., the lack of plasticity. Ductile iron is the material which retains all the advantages of cast iron, and at the same time allows obtaining the strength properties comparable or superior to the properties of heat-treated steels or cast steels.

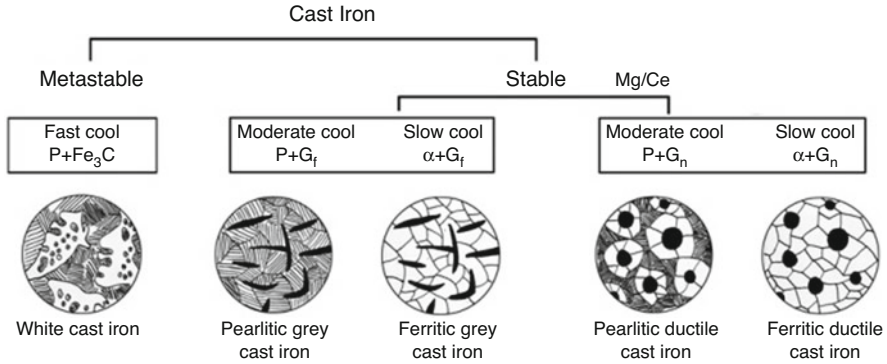


Fig. 5.2 Simplified classification of cast iron into different types depending on the type of solidification in a stable or metastable system; P pearlite, G_f flake shaped graphite, G_n nodule shaped graphite, α ferrite

5.1.2 Mechanical Properties

The main advantage of ductile iron is the unique combination of mechanical and plastic properties [15, 17, 18]. Comparing the minimum values of R_m (ultimate tensile strength) and A_5 (total elongation with 5 mm gauge length) obtained in conventional grades of this cast iron and in alloyed steel, carbon steel, and austempered ductile iron, the potential competitiveness of ductile iron with respect to steel deserves attention only in the case of the highest ductility (ductile iron with ferritic matrix) or highest strength (ductile iron with ausferritic matrix) (Fig. 5.3) [15]. From Fig. 5.3, it follows that austempered ductile iron (ADI) offers the properties which are a “continuation” of the cast steel properties in the direction of higher strength, while ADI grades with lower strength are competitive with the cast steel of the highest strength.

Compared to steel, another very important feature of cast iron is a 10% lower density. In combination with very high durability, it turns out that austempered ductile iron can be competitive not only to steel, but also to magnesium alloys and even aluminum alloys with respect to density (Fig. 5.4). Through small structural changes, such as the reduction of wall thickness, attempts to replace aluminum alloys with ADI have been successfully implemented [17]. The examples are available in various sources, e.g., in formation available on a website [17] about casting of a truck wheel hub of the same weight as an aluminum alloy casting (~ 15 kg) and which best proves this statement.

5.1.3 Vibration Damping Capacity

Subjected to cyclic loads, cast iron shows the ability to absorb the applied energy and convert it into heat resulting in fast damping of vibrations. The presence of

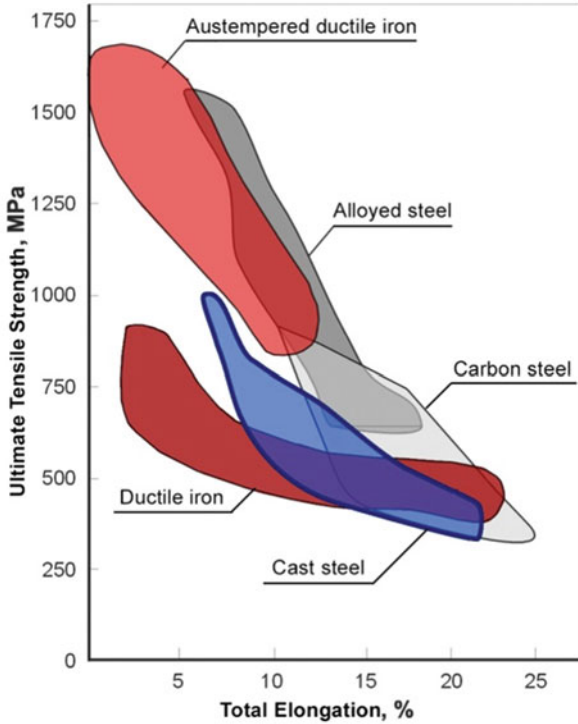


Fig. 5.3 Comparison of the achievable range of ultimate tensile strength and total elongation: austempered ductile iron, ductile iron, alloyed steel, carbon steel, and cast steel. (Author’s own analysis based on [14–17])

graphite in gray cast iron results in damping of vibrations faster than in steel (Fig. 5.5) [14, 15, 17]. This is of great importance in the case of unexpected or rapidly changing loads. Cast iron offers a faster relaxation of the accumulated stresses or suppression of vibration resonance which in other cases, even for materials of much higher strength, can prove difficult and, therefore, disastrous failure can occur.

The main structural constituent that affects the ability to damp vibrations is graphite. With increasing content and size of the graphite precipitates, this ability increases too. Therefore, in gray cast iron, the ability to dampen vibrations decreases with the increasing properties and structure refinement. For this property of cast iron, the metal matrix is incomparably less important, although much more effective damping of vibrations by the bainitic matrix of cast iron compared to the pearlitic matrix has been well documented [14]. The usefulness of gray cast iron for the production of gears can be explained by the fact that stresses arising at the base of the teeth, which is the place of stress accumulation, assume values much lower in the cast iron gears due to damping of vibration than in the steel gears.

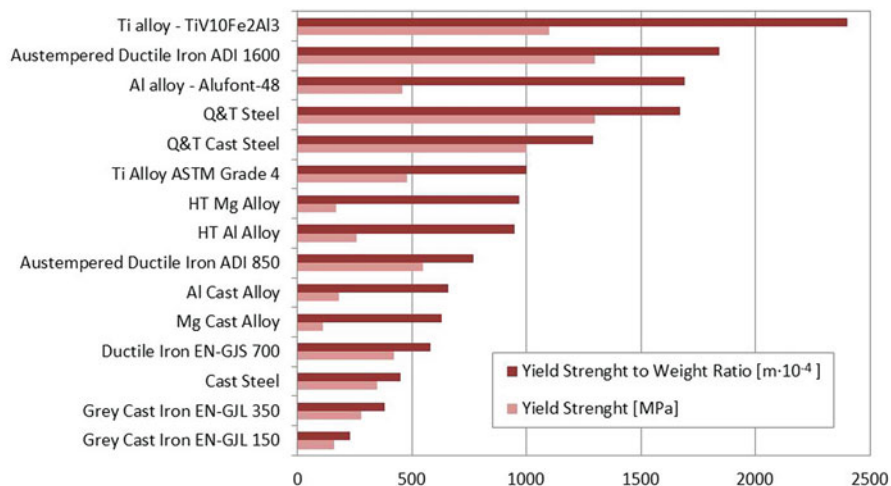


Fig. 5.4 Yield strength and the yield strength-to-weight ratio compared for selected materials from various cast irons, cast steels, and Al, Ti, and Mg alloys in different heat treatment conditions. Q&T – quenched and tempered, HT – heat treated, EN-GJL – gray iron grades according to European Standard EN 1561. (Author’s own analysis based on [1–17])

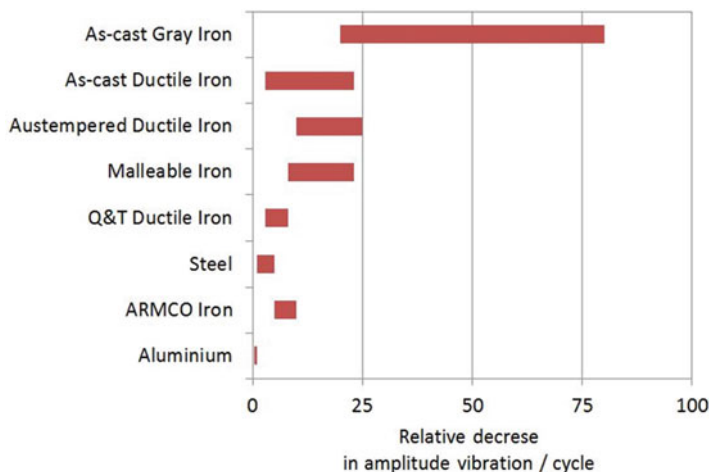


Fig. 5.5 Value of relative decrease in amplitude of vibration for different materials. (Author’s own analysis based on [14, 15, 17])

5.1.4 Manufacturing Costs

Cast iron is an attractive construction or structural material also in terms of its price, and not only when the cost of a kilogram of the product at current market prices in Europe is compared (Fig. 5.6) [13], but also when the cost of producing

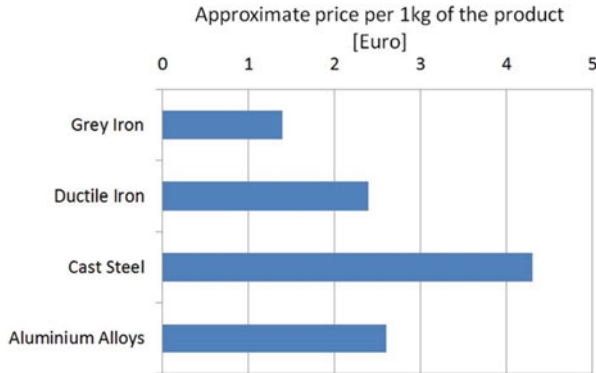


Fig. 5.6 Approximate price per 1 kg of the product for different materials (2018). (Author’s own analysis based on production sources)

Table 5.1 Energy consumption in the production of gears – a comparison of ADI castings and steel forgings [17]

Operation	Energy consumption, kWh/t	
	ADI	Steel
Making semifinished products	2500	4500
Annealing	–	500
Austempering	600	–
Carburizing	–	800–1200
Total	3100	5600–6200

complex geometries from different materials with the same properties is compared. An interesting example is the comparison of manufacturing costs of products made from carburized steel and cast from ADI which serves as parts of a machine operated under dynamic mechanical loads and friction conditions (Table 5.1) [17]. The documented almost 50% savings in costs related to energy consumption is not the only advantage of technology conversion in this particular case. Other benefits include reduction of product weight by almost 10%, reduction of noise during operation, almost three times higher durability of castings, and six times higher durability of cutting tools, resulting mainly from the ductile iron machinability before the heat treatment process [17].

5.2 Types of Cast Iron

High-quality alloys are construction materials whose production complies with all technological standards leading to a product without defects with properties that meet the minimum standards. This is also true in the case of iron castings. This study is largely devoted to the problem of the structure and structure-related properties, and not to the quality of the technological process, which should always be at the

highest level. However, it should be remembered that the type of structure formed during casting solidification and cooling process will have a significant impact on the properties of this casting, also in the case of the most-advanced cast iron grades subjected to heat treatment.

5.2.1 Production – Cast Iron Structure

The structure of cast iron can be shaped in a number of different ways. The melt “refining” processes, the solidification conditions and cooling rate, or control of the chemical composition are the most important factors, which when properly selected and monitored will make the control of cast iron properties possible. Therefore, even a very brief discussion of these issues is extremely important to capture the differences between cast iron and steel in which the postcasting structure is only of minor significance.

According to the earlier definition, cast iron is composed not only of iron and carbon, but also of a number of other elements that always exist in this alloy and include silicon, manganese, phosphorus, and sulfur. Other elements such as Cu, Ni, Mo, or Cr are usually regarded as additional alloying additives. Each of them exerts a greater or lesser influence on the course of primary and eutectic crystallization, and this influence should always be considered taking into account the content of individual elements and cooling conditions. Chemical composition has a very complex effect on the structure of cast iron [20–23] although in this complex system it is carbon that plays an overriding role in shaping the cast iron microstructure.

Carbon is the main constituent determining the casting, mechanical, and functional properties of cast iron [2]. According to the binary Fe-C phase equilibrium diagram, the cast iron in a stable system contains at least 2.08 wt.% C (Fig. 5.7) [14, 16]. However, since it always contains a certain amount of Si and P, the critical carbon content can vary within a fairly wide range. Due to the strong effect of silicon and phosphorus on the carbon content at the eutectic point with a tendency to bring this content to lower values, in practice the so-called carbon equivalent C_E is used [24]. It is a measure of the deviation of the chemical composition of cast iron of its eutectic composition and is defined as follows:

$$C_E = C + \frac{\text{Si} + \text{P}}{3} \quad (5.1)$$

where C, Si, and P contents are in wt.%. Establishing this value with respect to the eutectic value of 4.26 wt.% C enables dividing the cast iron into three groups, i.e., hypoeutectic ($C_E < 4.26$), eutectic ($C_E = 4.26$), and hypereutectic ($C_E > 4.26$) [14, 19]. Among them, the most popular in industrial practice is the hypoeutectic cast iron, mainly due to the possibility of obtaining a wide range of in-service properties. From a production point of view, it is also important whether the cast iron solidifies in a stable or metastable system. The metastable system is associated

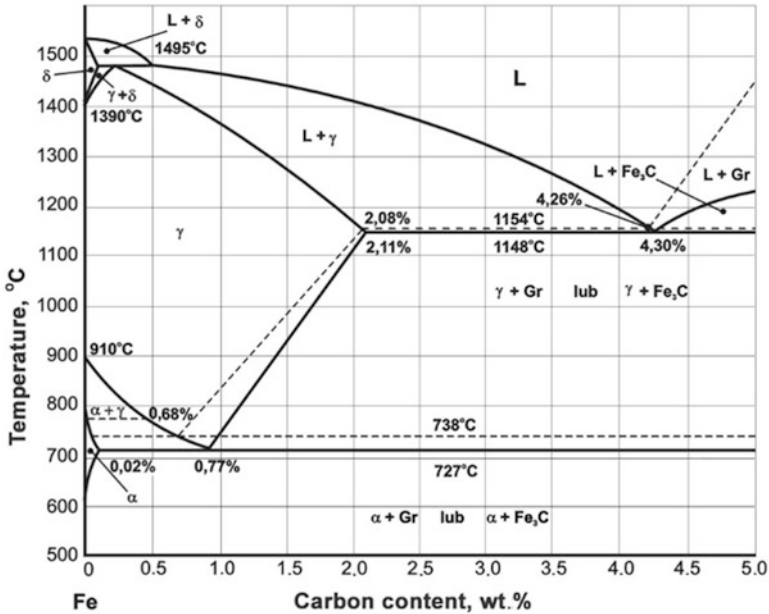


Fig. 5.7 Phase equilibrium diagram of Fe-C alloys: thin line – Fe-C graphite system; thick line – Fe-Fe₃C system; L – liquid solution; δ – high-temperature ferrite; γ – austenite; α – ferrite; Gr – graphite. (Based on [14, 16])

with the formation of hard and brittle cementite eutectic, while stable system ensures the formation of graphite eutectic with precipitates of free graphite. This type of cast iron is the most widespread and worldwide-appreciated casting material for structural applications. In a further part of this chapter, this material will be the main subject of discussion.

An ideal cooling curve and true cooling curve from the liquid of the hypoeutectic gray cast iron have several differences between the two runs (Fig. 5.8). First, there is a more or less visible characteristic “isothermal arrest”. According to Karsay [25], its origin on the true curve is identified with undercooling below the equilibrium temperature due to which a “driving force” appears in the system to carry into effect the nucleation of the primary phase, which in the case of hypoeutectic cast iron is austenite. The rate of solidification at this point becomes quite significant, trying to compensate for some delay caused by the need to achieve sufficient undercooling of the liquid alloy. Acceleration of solidification during this period leads to an increase in temperature in the direction of the equilibrium freezing point, which results in the effect visible in Fig. 5.8. As a result of further cooling, the alloy reaches its eutectic temperature. Triggering the eutectic transformation also requires some undercooling below the equilibrium temperature. Due to the simultaneous formation of graphite and austenite, the temperature rises again, generating the phenomenon called *recalescence* [14, 25]. Depending on the cooling rate, the recalescence can

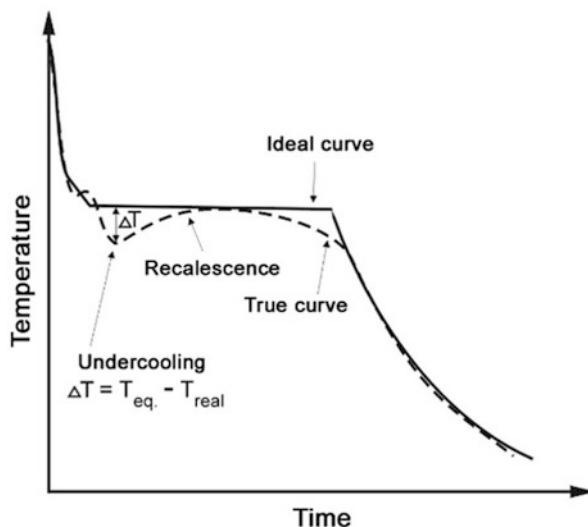


Fig. 5.8 Typical run of the ideal and true cooling curve of hypoeutectic gray iron. (Based on [25])

make the solidifying eutectic cast iron reach the equilibrium temperature or remain below this point. Further cooling is associated with the completion of solidification – first by one phase (graphite) and later by another phase (austenite) [14]. This phenomenon evokes some deviations from the ideal cooling curve with a tendency toward continuous lowering of the temperature.

The above-discussed solidification sequence of the hypoeutectic gray cast iron, which results in the formation of a primary phase in the form of austenite dendrites spread against the background of graphite eutectic, is only partly true, and this is due to the fact that solidification in the systems comprising an eutectic point takes place under the conditions of so-called competitive growth of two phases. As a consequence, in the eutectic systems, the type of microstructure depends not only on the chemical composition of the alloy but also on the rate of growth of the eutectic mixture and the primary (preeutectic) phase. This means that if the growth rate of the eutectic is higher than the growth rate of the primary phase, the obtained microstructure will be fully eutectic. The above is related to the concept of the coupled zone of eutectic growth, which is understood as a range of the alloy chemical composition, growth velocity, and temperature gradient, ensuring the formation of a completely eutectic microstructure – without primary phases, both pre- and posteutectic. Disregarding any more detailed studies of the eutectic solidification, which are described in the works of Campbell and Fraš [18, 24], it should be noted that due to the chemical composition of cast iron approaching the eutectic composition and the above-discussed conditions of coupled eutectic growth, the microstructure of cast iron is usually fully eutectic and its dendritic character is recognizable even after long-term heat treatment processes (Fig. 5.9).

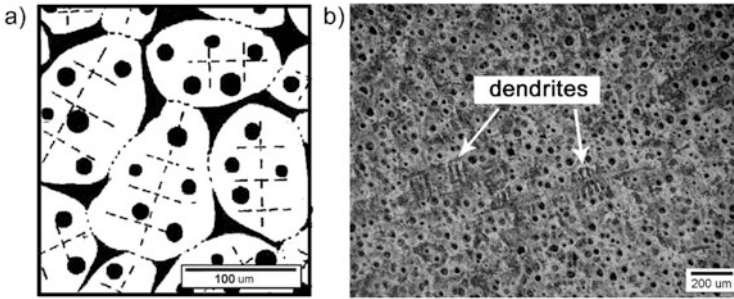


Fig. 5.9 Model of the primary structure of ductile iron: (a) – model of structure; black fields between cells are the last to freeze regions (LTF), dashed lines denote dendrite arms; (b) optical microscopic photo of ADI – Nomarsky contrast. (Author’s own work)

According to the phase equilibrium diagram of Fe-C alloys (Fig. 5.7), at room temperature, two basic phases containing no alloying additions can coexist in hypoeutectic gray cast iron. These are the following phases: solid carbon solution in α iron (ferrite) and graphite (stable system). Alloyed or heat-treated cast iron may also contain solid solution of carbon in γ iron (austenite) and product of diffusion-free transformation (martensite). On the other hand, individual constituents of cast iron can give rise to the formation of two- or three-phase structural constituents, such as various types of eutectic (graphite, cementite) and pearlite or bainite. Studies of the cast iron microstructure after casting and cooling at different speeds to ambient temperature showed the possibility of the formation of different phases in the ductile iron matrix. The research presented by Rivera [26] indicates the possibility of obtaining a wide range of matrix types from martensitic, through austenitic-ferritic and pearlitic up to ferritic in nonalloyed cast iron or in cast iron with low additions of Ni < 1 wt.%, Cu < 0.7 wt.% and Mo < 0.15 wt.%.

Reducing the wall thickness is tantamount to increasing the casting solidification and cooling rate, and thus to increasing the homogeneity of the concentration of elements in cast iron [27]. However, as shown in [28, 29], as the wall thickness increases, the number of graphite precipitates in the casting decreases. This promotes the microsegregation of elements, and thus the reduction of mechanical properties. In turn, a large number of precipitates in the case of a high solidification rate (smaller wall thickness) means smaller distance between graphite precipitates, and hence higher chemical homogeneity in microregions. The mechanical properties were found to be much better in ductile iron castings with thinner walls, than in the slowly solidifying castings characterized by large and sparsely distributed graphite nodules [30, 31].

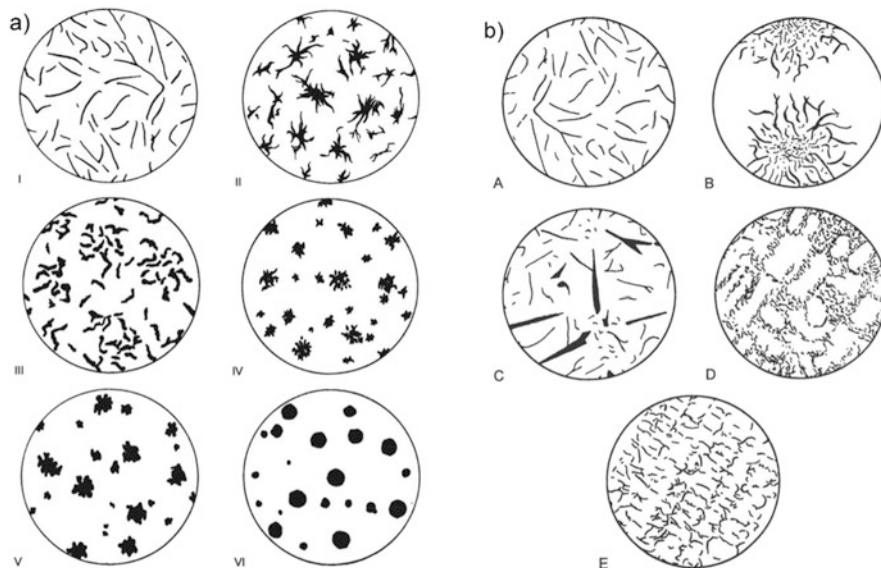


Fig. 5.10 Graphite classification by visual analysis as per International Standard ISO 945-1:2017 (E): (a) reference images for principal graphite forms in the cast irons from flake to nodular shape (forms: I, II, III, IV, V and VI), (b) reference images for graphite distribution (type A: random flake graphite in a uniform distribution, type B: rosette flake graphite, type C: kish graphite (hypereutectic compositions), type D: undercooled flake graphite, type E: interdendritic flake graphite (hypoeutectic compositions)). (Based on [14])

5.2.2 Graphite Morphology

Different forms of graphite (flake, nodular, vermicular, chunky, exploded, coral, etc.) occurring in the cast iron determine its properties (Fig. 2.4), but it was the discovery of the possibility of making the graphite grow in a spherical form during the gray cast iron solidification that has opened the way for foundry men not only to eliminate the inherent brittleness of cast iron, but also to obtain the strength properties competing with the best grades of steel (Fig. 5.10).

The following factors determine the graphite form in the cast iron: the type and structure of nuclei, physicochemical factors, and growth conditions in the directions perpendicular to the graphite crystal walls. According to many scientists [14, 18, 24], the morphology of graphite precipitates is probably most affected by variations in the speed of crystal growth in different directions, related to both the internal structure of graphite and external factors. The most important role is attributed to elements which introduced even in small amounts can clearly change the shape of graphite precipitates. Thus, Mg, Ce, and other elements promote the formation of nodular graphite, while Sb, Pb, Al, S, Ti, and Bi facilitate the crystallization of flake graphite. So far, the mechanism of interaction of these elements has not been fully explained, but it is known that they exert different effects on the growth rate of

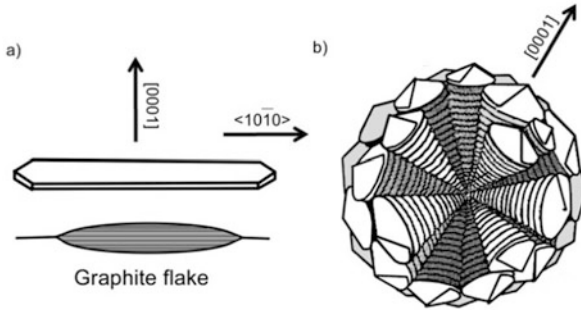


Fig. 5.11 Schematic presentation of (a) growth of graphite flake and (b) graphite nodule as a polycrystal composed of conically coiled layers. (Based on [14])

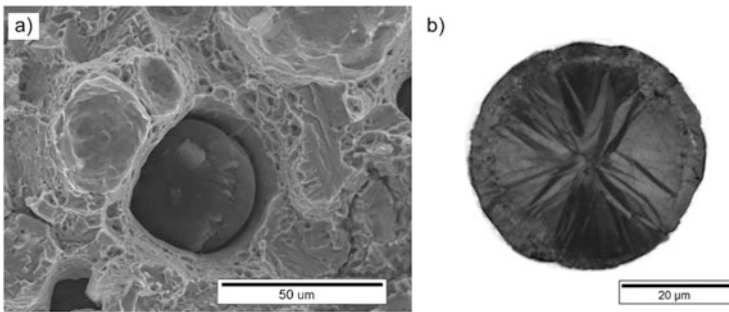


Fig. 5.12 (a) Scanning electron microscope (SEM) image of nodular graphite in an ausferritic matrix, (b) light microscope (LM) image of the cross-section through a graphite nodule. (Author's own work)

graphite crystals in $[0001]$ and $\langle 1010 \rangle$ directions. It is assumed that these elements may be incorporated into the lattice of graphite or may be selectively absorbed on the walls of the growing crystal. It seems highly probable that the spheroidizing elements facilitate the formation of $\langle 1010 \rangle$ dislocations, which promote the growth of graphite crystals in $[0001]$ direction but inhibit this growth in direction. From Fig. 5.11 [14] presenting the growth of graphite structure, it follows that graphite flakes in gray cast iron are monocrystals (often bent and branched), while nodular graphite precipitates are polycrystals (Fig. 5.12).

In contrast to other types of gray cast iron described in the literature [14, 24, 25], the essence of the solidification of ductile iron is in the special crystallization mode of graphite in the form of nodules. This graphite crystallizes directly from the liquid, where its nucleus in the initial stage grows freely as a specific preeutectic phase and takes on a spheroidal form (Fig. 5.11). The nuclei grow in the space between the arms of the austenite dendrites formed earlier. This location promotes the heterogeneous nucleation of the eutectic austenite grains. Austenite grows around the graphite nodule until its complete closure, contrary to flake graphite whose

Fig. 5.13 Schematic presentation of the growth of (a) flake and (b) nodular graphite in a eutectic system with austenite. (Based on [14])

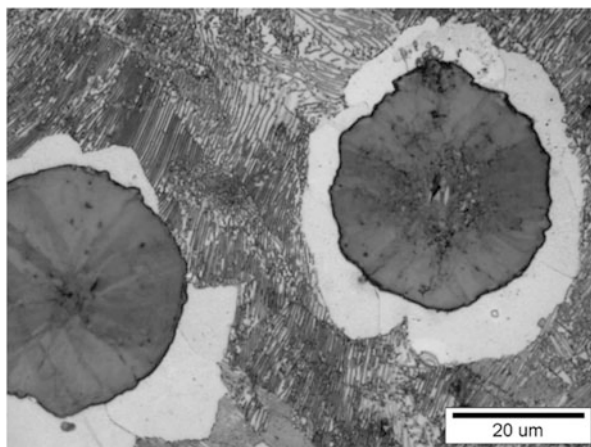
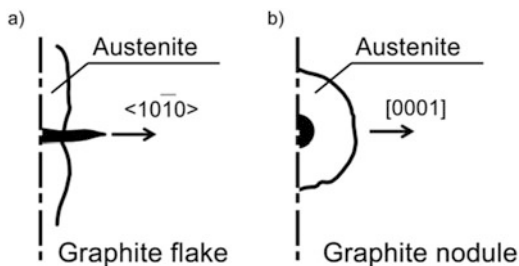


Fig. 5.14 Two neighboring eutectic cells in the ductile iron with a pearlitic-ferritic matrix. (Author's own work)

growth precedes the build-up of austenite (Fig. 5.13) [14], forming a notch stress at the tip of a sharp precipitate. After losing contact with the liquid, the growth of the nodule takes place through the diffusion of carbon from the surrounding austenite. Together with the austenite envelope, after solidification the flake or nodular graphite forms a characteristic structure commonly known as eutectic cell (Fig. 5.14). From now in this chapter, the product of eutectic transformation in the form of a mixture of phases will be referred to as a eutectic cell.

5.2.3 Influence of Chemical Composition – Microsegregation

The primary microstructure of ductile iron is one of the most important factors affecting the final properties of cast iron in both as-cast state and after heat treatment (or after other technological treatments). Therefore, its shaping through properly chosen chemical composition, and especially striving for maximum microstructural

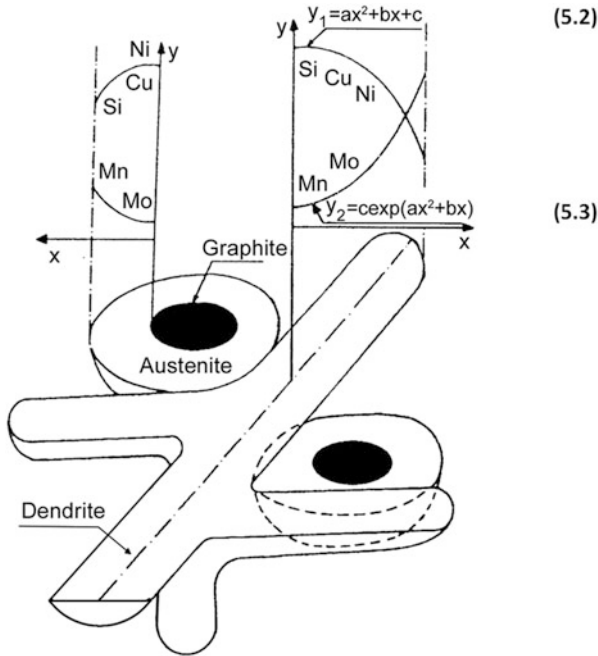


Fig. 5.15 Diagram of ductile iron structure and microsegregation of its constituents. Eq. (5.2) $y_1 = ax^2 + bx + c$; Eq. (5.3) $y_2 = cexp(ax^2 + bx)$. (Based on [21])

homogeneity of the distribution of elements in a volume of the alloy, is of particular importance in the overall production process.

When analyzing the microstructure of ductile iron after solidification, it is convenient to use the model shown in Fig. 5.15 [21]. As demonstrated by Sękowski and Pietrowski [21, 23], a specific type of microsegregation occurs in cast iron, described by Eq. (5.2) for noncarbide forming elements and by Eq. (5.3) for carbide-forming elements (Fig. 5.15). Microsegregation raises the concentration of molybdenum, manganese, and carbon at grain boundaries and causes enrichment in silicon, nickel, and copper in areas close to graphite nodules. This has its reflection in the changes that occur when the structure becomes so complex as it starts cooling down to ambient temperature. The elements present in cast iron, having a definite influence on the formation of individual phases, also interact with each other, weakening or strengthening the corresponding transformations. For example, high silicon content promotes carbon activity, while Cu and Ni counteract the carbide-forming tendency of molybdenum. However, it should be remembered that microsegregation, which is a diffusion-controlled process and depends primarily on the cooling rate, is also a function of the size of graphite nodules and internodular spacing. In turn, the cooling rate affects not only the speed, and hence the extent of diffusion, but also the degree of dispersion of phases and structural constituents.

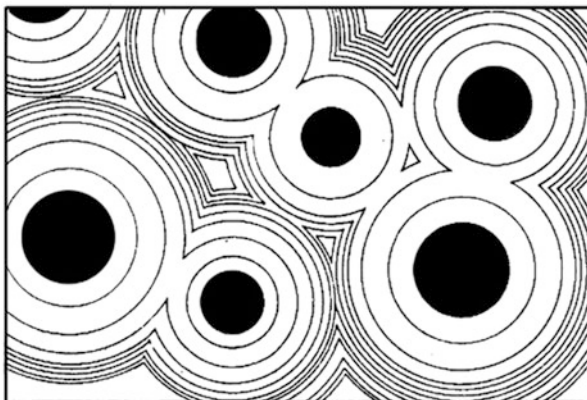


Fig. 5.16 Concentration model of an idealized eutectic cell and ductile iron structure: lines of equal concentration of manganese. (Based on [23])

Adopting Sękowski's idealized model of ductile iron microstructure as a set of eutectic cells [23], one can illustrate in a simplified way the microsegregation of individual elements (Fig. 5.16). It is easy to notice that microsegregation will be significantly affected by the distance between adjacent graphite nodules. Hence it follows that the refinement of nodular precipitates of graphite and an increase in their number should be the main technological guidelines in an attempt to reduce the intensity of the microsegregation of elements in ductile iron. The presence of a given element in an appropriate concentration or absence of this element also contributes to changes in the intensity of the microsegregation in cast iron. However, in terms of the microstructure homogenization, the most problematic is control of the increasing concentration of elements at the boundaries of austenite dendrites or eutectic cells [32]. Proportionally, heterogeneity occurs in the mechanical properties transferred from the microscale (e.g., different properties at the boundaries and in the centre of eutectic cells) to the macroscale, determining the properties of finished castings through different structures formed in the matrix of cast iron.

5.2.4 Importance of As-Cast Matrix Microstructure

As already discussed, the microstructure of gray cast iron is composed of graphite embedded in a metal matrix. Although the degree of spheroidization, and the size and distribution of graphite precipitates are extremely important features, the type of cast iron matrix is undoubtedly equally important. A ferritic, ferritic-pearlitic, pearlitic, martensitic, or bainitic matrix surrounding the graphite precipitate is the result of various treatments used by the foundry men to obtain the desired properties of cast iron during solidification and cooling. Appropriate control of chemical composition is the simplest method that allows obtaining practically all of the above mentioned types of microstructure.

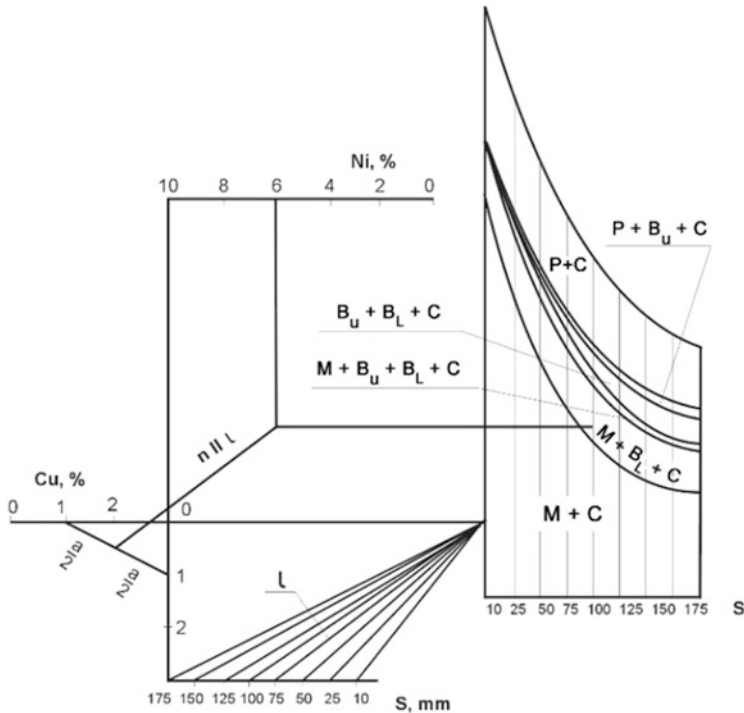


Fig. 5.17 Synergistic influence of Ni, Mo, and Cu and casting wall thickness “S” on the microstructure of ductile iron in as-cast state at a constant content of 3.4 ± 0.10 wt.% C, 2.75 ± 0.10 wt.% Si, 0.35 ± 0.05 wt.% Mn, 0.045 ± 0.005 wt.% Mg. *C* molybdenum carbides, *P* pearlite, *F* ferrite, *B_U* upper bainite, *B_L* lower bainite, *M* martensite. (Based on [20])

Microstructures that provide the highest strength properties, i.e., bainitic, pearlitic, or martensitic, are easy to obtain after casting by application of special technological treatments. For example, the addition of an appropriate amount of nickel to ductile iron produces a wide range of microstructures even in the as-cast state [20, 34]. A double or triple combination of Ni, Cu, or Mo as alloying additives can produce similar effects, but it must be economically viable. Therefore, the method of obtaining the required as-cast microstructure, and thus the required properties, through the introduction of a significant amount of alloying additives is usually applied to castings massive or with intricate shapes, in the case of which the heat treatment is either difficult or even impossible. In several studies presented by Pietrowski [20, 21, 32], a detailed description of the type of microstructure obtained by adding an appropriate amount of alloying constituents to ductile iron was provided. The nomogram in Fig. 5.17, developed as the result of extensive research, perfectly reflects the possibilities of using the above-mentioned treatments. It directly indicates that for the decreasing wall thickness, the range of bainitic

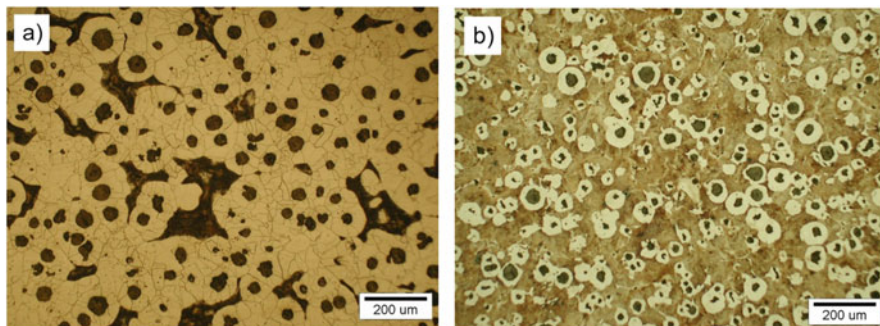


Fig. 5.18 (a) Ferritic-pearlitic and (b) pearlitic-ferritic matrix in ductile iron. (Author's own work)

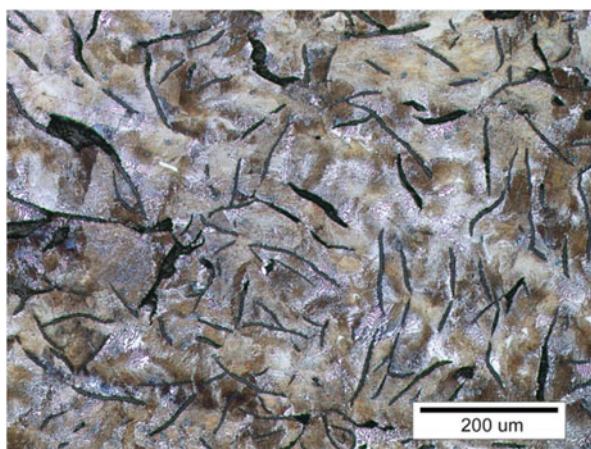


Fig. 5.19 Pearlitic matrix in gray cast iron with flake graphite. (Author's own work)

microstructure with the best mechanical properties narrows, while the range of the bainitic-martensitic or martensitic microstructure becomes wider.

The functional properties of castings depend to a large extent on the type of metal matrix present in ductile iron. In terms of the matrix type, the ductile iron is divided into austenitic, ferritic, ferritic-pearlitic, or pearlitic. The matrix may also comprise bainite, ausferrite, or tempered martensite. However, controlled solidification and cooling of ductile iron usually shape its matrix as a mixture of pearlite and ferrite (Fig. 5.18). In the as-cast state, the fully pearlitic matrix is obtained either by sufficiently rapid cooling or, in the case of castings with thick walls, by introducing pearlite-forming alloying elements, such as Cu, Sn, Cr, or Ni (Fig. 5.19). Due to them, immediately after casting, the highest ductile iron grades are produced (Table 5.2) [25, 36, 37]. To obtain yield strength above 420 MPa it is necessary to either introduce a certain amount of alloying elements to the ductile iron or carry out an appropriate heat treatment [16].

Table 5.2 Designation and mechanical properties of selected cast iron grades with flake and nodular graphite according to European standards. (Based on [25, 36, 37])

Cast iron designation	Yield strength [MPa] (min.)	Tensile strength [MPa] (min.)	Total elongation [%] (min.)	Microstructure of metallic matrix
Flake graphite cast iron				
EN-GJL-150	98	150	0.3	Ferritic – pearlitic
EN-GJL-200	130	200	0.3	Pearlitic
EN-GJL-250	165	250	0.3	Pearlitic
EN-GJL-300	195	300	0.3	Pearlitic
EN-GJL-350	228	350	0.3	Pearlitic
Nodular graphite cast iron				
EN-GJS-350-22	220	350	22	Ferritic
EN-GJS-400-18	250	400	18	Ferritic
EN-GJS-450-10	310	450	10	Ferritic – pearlitic
EN-GJS-500-7	320	500	7	Pearlitic – ferritic
EN-GJS-600-3	370	600	3	Pearlitic – ferritic
EN-GJS-700-2	420	700	2	Pearlitic
EN-GJS-800-2	480	800	2	Pearlitic or martensitic
EN-GJS-900-2	600	900	2	Martensitic
Austempered ductile iron (nodular graphite)				
EN-GJS-800-10	500	800	10	Ausferritic
EN-GJS-900-8	600	900	8	Ausferritic
EN-GJS-1050-6	700	1050	6	Ausferritic
EN-GJS-1200-3	850	1200	3	Ausferritic
EN-GJS-1400-1	1100	1400	1	Ausferritic

Heat treatment can totally remodel the matrix structure without affecting the graphite precipitates in gray cast iron. It is usually applied to correct the microstructure (e.g., to dissolve carbides) or to improve the required properties of the casting (e.g., to increase hardness). However, heat treatment must always be economically justified. The correct cast iron microstructure should normally be obtained immediately after casting, but if for some reason it is not possible to provide in this way the desired properties or the customer explicitly wishes a specific type of the heat treatment to be performed on the cast iron, the heat treatment must be carried out in order to obtain a pearlitic, martensitic, or ausferritic matrix. This aspect of the ductile iron heat treatment is taken into account when the austempered ductile iron is produced. The process of making castings from this material has opened a new chapter in the production of cast iron as a technology having undoubtedly its place in the “high-tech” row. This is well illustrated by the division of cast iron grades with respect to graphite shape and matrix type according to European standards (Table 5.2).

5.3 Modern Heat Treatment of Cast Iron

The microstructure formed during solidification and cooling has a fundamental effect on the properties of cast iron. Searching for higher strength and plasticity or adding special properties to cast iron is the reason why heat treatment has become a very important factor in the development of the production of iron castings.

Due to the discovery of the nodular form of graphite, cast iron was started to be perceived as a plastic material and for a long time the heat treatment was considered unnecessary, especially that it considerably increased production costs. This is particularly well visible on the example of malleable cast iron, where long-lasting (>30 h) high-temperature annealing gives the same properties as the properties obtained in as-cast ductile iron. Heat treatment primarily affects the gray cast iron matrix, so it should be remembered that only with the nodular shape of graphite one can take full advantage of the microstructure modification. Although heat treatment is also carried out on gray iron castings with flake graphite or vermicular graphite, these are still only scientifically important processes.

5.3.1 Normalizing and Toughening

Normalizing, hardening, and toughening are carried out to increase the strength and resistance to wear. All these thermal processes have been known and used for decades but due to their existence; today modern cast iron grades are often obtained, e.g., by incorporating a conventional thermal cycle into innovative heat treatment [34]. Heat treatment is also applied for technological reasons as a means to get a homogeneous postcast structure in castings or to reduce the residual stresses to minimum.

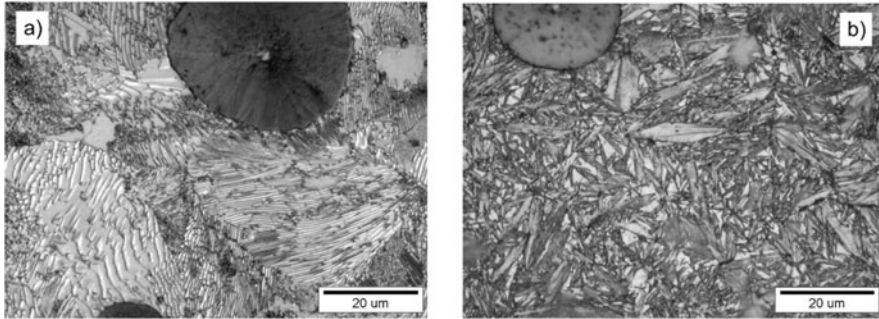


Fig. 5.20 Pearlitic (a) and martensitic (b) matrix of ductile iron. (Author's own work)

The outcome of “normalizing” is homogenization of the chemical composition and obtaining a matrix composed of highly dispersed pearlite (Fig. 5.20a). The treatment consists in annealing castings at a temperature higher by approximately 80 °C than the critical temperature (820–900 °C for gray cast iron and 870–925 °C for ductile iron) followed by rapid air cooling. The rapid air cooling treatment can be applied immediately after casting by knocking out the cast item from the foundry mold. In this way, higher strength and hardness are obtained. Normalizing is often required to dissolve carbides or to reduce the microsegregation of elements in castings with thick walls.

“Toughening” is applied when castings are expected to offer the yield strength and elongation higher than the standard grades, including grades after normalizing treatment, e.g., EN-GJS-800-2. This type of heat treatment is based on quenching followed by tempering. Tempering also removes quenching stresses and improves fracture toughness.

Rapid cooling ensuring the austenite → martensite transformation is usually carried out in an oil bath from the casting annealing temperature, i.e., from the temperature higher by 30–100 °C than the critical temperature, for a time depending on the type of cast iron. The presence of graphite distinguishes cast iron from steel and makes the holding time longer. The time taken by the austenite to get saturated with carbon amounts to about 10 min for the cast iron with ferritic matrix and flake graphite and up to 80 min for the cast iron with nodular graphite [14]. The shorter the time, the higher is the temperature of annealing and the larger is the graphite-austenite interface, i.e., the finer are the precipitates of graphite. In a pearlitic matrix, the complete transformation into austenite will proceed faster than in the ferritic matrix. For these reasons, the hardness of cast iron is much more sensitive than the hardness of steel to the time and temperature of annealing prior to quenching. The presence of graphite-austenite phase boundaries and surface development also affect the rate of matrix transformation into austenite. Therefore, gray cast iron with flake graphite shows lower hardenability than the spheroidal graphite cast iron of the same chemical composition.

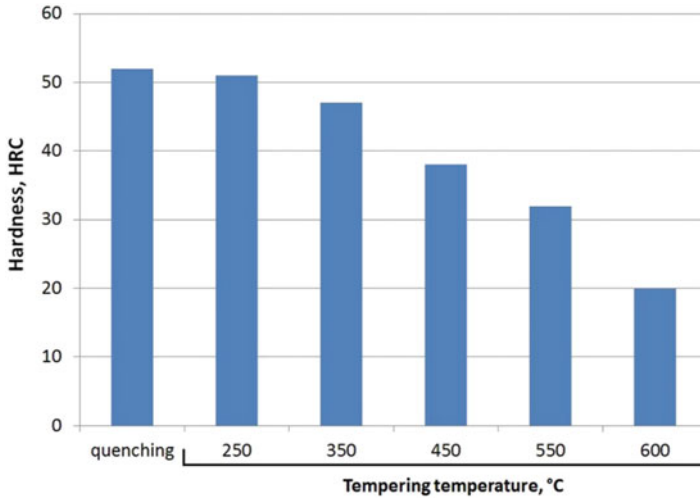


Fig. 5.21 Hardness of cast iron as a function of tempering temperature. (Based on [14, 35])

Quenching produces a martensitic matrix, providing high hardness levels to the castings (Fig. 5.20b), but it is tempering that ultimately shapes the final properties of castings, which largely depend on the time and temperature of this treatment. When high hardness and abrasion resistance are required, castings are subjected to low-temperature tempering (180–250 °C). On the other hand, high fracture toughness requires tempering carried out at high temperature (550–650 °C) (Fig. 5.21) [14, 35]. After these processes, slow cooling to ambient temperature is recommended to minimize the level of internal stresses. A special feature of cast iron tempered at a temperature above 500 °C is the occurrence in the structure of a new constituent, namely the secondary graphite [35]. It has the form of small spheroids evenly distributed in the matrix.

5.3.2 Austempering of Cast Iron

Austempering of cast iron is primarily the heat treatment of ductile iron; hence the product has the well-known name austempered ductile iron (ADI). Other types of gray cast iron, i.e., with vermicular or flake graphite, are also subjected to this treatment for better resistance to wear or fracture toughness [16, 31]. In this part of the chapter, however, the description of ADI will prevail, bearing in mind the fact that it is the cast iron most popular in today's research.

ADI is a construction material that still arouses the curiosity of scientists and the interest of practitioners. Perhaps that is why new ideas and scientific research aimed at further improvement of its properties still appear [14, 15]. This is particularly important in the aspect of the ADI implementation into practical use. It is enough to

mention that since 2000 the production of this casting material in the world has been increasing at a rate of several tens of thousands of tons per year [16]. This proves the great interest in ADI of the casting users who see the opportunity to make from this material a large variety of parts of machinery and equipment operating in the automotive, railway, agricultural, and defense industries.

Austempered ductile iron is classified according to European and American standards [36, 37]. A characteristic feature of this material is the combination of high plastic and mechanical properties, comparable to many grades of steel. It has high mechanical properties owing to the properly conducted heat treatment, which consists of austenitizing and austempering operations. Both these operations are extremely important from the point of view of changes occurring in the microstructure over time and reflected in the changing properties of ADI. Austenitizing primarily determines the carbon content in austenite, while austempering following rapid cooling from the austenitizing temperature ultimately shapes the mixture of ferrite and austenite called ausferrite. The term *ausferrite* was first used in Poland at the 20th Steel Casters Conference in Raba Niżna, 1997 [16]. Ausferrite with a specific morphology and proportions of individual phases at ambient temperature is the mixture responsible for ADI properties (Fig. 5.22).

The process of heat treatment of ductile iron seems to be very simple with regard to both performance and desired effects. However, as the research shows [33], it is not always possible to meet the minimum property criteria specified by the standard. In the context of this study, it seems interesting to accurately present the kinetics of the formation of phases in ADI together with their characteristics.

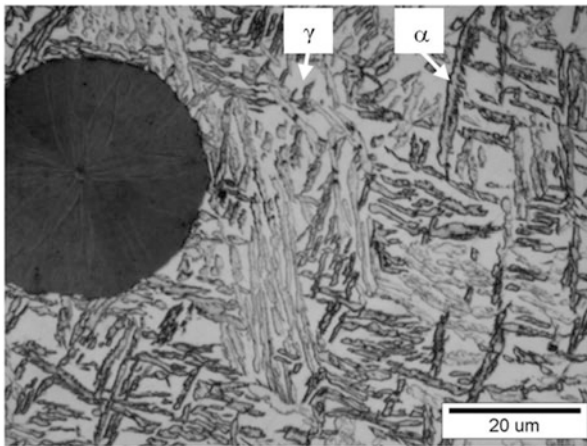


Fig. 5.22 Typical microstructure of austempered ductile iron (ADI). γ austenite, α ferrite plates. (Author's own work)

5.3.2.1 Austenitizing

Both temperature and time of the austenitizing treatment exert a significant effect on the carbon content in the austenite which forms around the graphite nodules in cast iron. The content of carbon determines the course of subsequent heat treatment and, as a consequence, affects the mechanical properties of cast iron.

By temperature setting it is possible to adjust the value of the equilibrium carbon concentration in austenite, while time decides if and when this equilibrium occurs. The higher the austenitizing temperature, the faster is the process of the carbon saturation in austenite. The solubility of carbon originating from graphite particles also increases. Austenite becomes more homogeneous and its grains start growing [38].

The relationship between austenitizing temperature and carbon content in austenite is well known [29]. For Fe-C-Si alloys, this value can be calculated from equation [29]:

$$C_{\gamma}^A = \frac{T_A}{420} - 0.17(Si) - 0.95 \quad (5.4)$$

where

C_{γ}^A – carbon content in austenite at austenitizing temperature in wt.%

T_A – austenitizing temperature [°C]

Si – content of the alloy is also in wt.%

Using this equation, a graph was developed showing influence of the austenitizing temperature T_A on carbon concentration in γ iron (Fig. 5.23). The graph is consistent with the experimental results [40].

With a sufficiently long time of austenitizing, an equilibrium carbon content can be obtained in the resulting austenite. There is no doubt that longer time of austenitizing makes the distribution of alloying elements in austenite grains more homogeneous and may contribute to the decomposition of carbides occurring in the microstructure of cast iron.

Both chemical composition and initial microstructure of cast iron are very important factors determining the effectiveness of austenitizing process. The pearlitic matrix of cast iron allows for faster C saturation in austenite than in the ferritic matrix. The factor responsible for this phenomenon is the difference in the kinetics of the transformation of pearlite and ferrite into austenite. The rate of C saturation in austenite also depends on the size and distribution of graphite nodules present in the microstructure. The larger the volume of graphite nodules and the smaller the distance between them, the shorter is the time needed by the austenite to get saturated with carbon. With the small internodular spacing, austenite will achieve the equilibrium carbon concentration in a shorter time. In addition to carbon, the most important constituent of cast iron is silicon. Its task is not only to reduce the carbon content in saturated austenite, but it also increases the temperature of

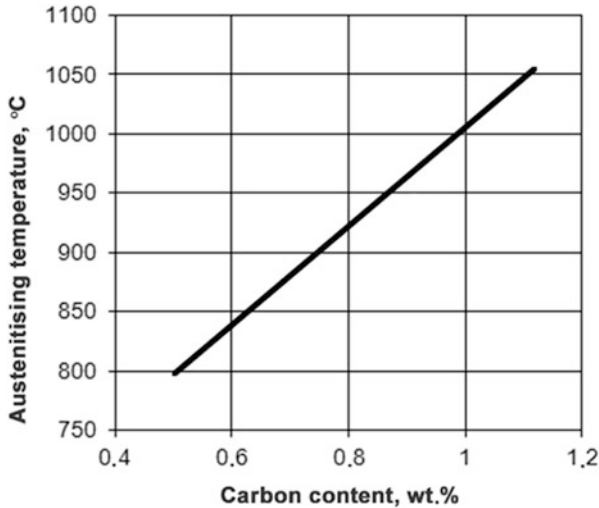


Fig. 5.23 Graph illustrating the relationship between austenitizing temperature and maximum carbon content in austenite. Carbon concentration in austenite calculated from Eq. (5.4) for the silicon content of 2.65 wt.%. (Based on [20, 40])

eutectoid transformation and extends the critical temperature range. Chromium also increases this temperature, whereas manganese and nickel reduce its value [18]. The presence of copper and nickel in cast iron has some influence on the austenitization process. Saturation of austenite with carbon depends on time and proceeds most intensely in the initial stage of this process. Cast iron containing nickel and copper takes longer time to reach the equilibrium carbon concentration in γ iron. However, studies conducted by Darwish and Elliott suggest that it is the austenitizing temperature and not the presence of alloying elements that is most critical in achieving the equilibrium carbon content in austenite [41].

In practice, austenitizing of cast iron is carried out in the temperature range of 850–930 °C, i.e., at a temperature by about 30–100 °C higher than the critical temperature (upper limit in the temperature range of eutectoid transformation). During heat treatment of ductile iron, the austenitizing temperature T_A is usually selected taking into account the microstructure of cast iron. The selected time of treatment depends on the chemical composition of cast iron and casting microstructure before austenitizing, based on the casting wall thickness, typically in the range of 48–150 s per 1 mm of the raw casting wall section [30].

5.3.2.2 Austempering

After austenitizing, austempering is carried out, i.e., rapid cooling of the casting to the temperature at which the isothermal transformation takes place (Fig. 5.24). The process starts with the nucleation and growth of ferrite plates forcing carbon

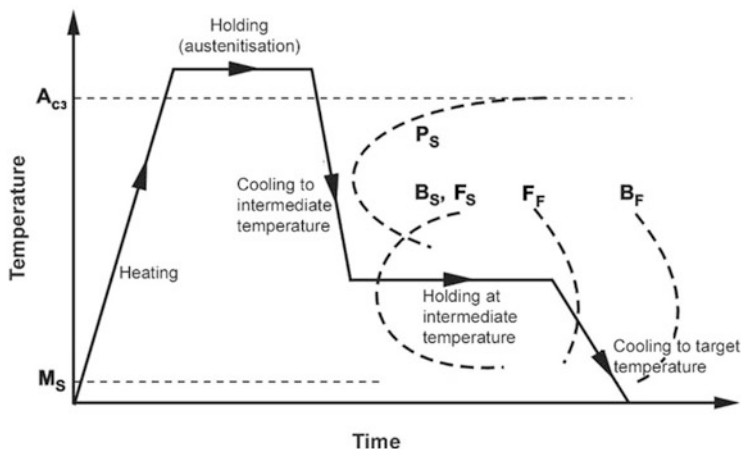
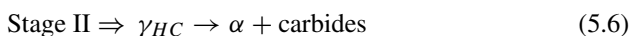
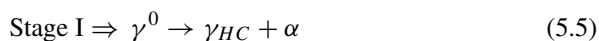


Fig. 5.24 Schematic diagram showing heat treatment steps during production of austempered ductile iron; P_S the beginning of pearlite transformation, B_S , B_F the beginning and end of bainite transformation, respectively, F_S , F_F the beginning and end of ausferrite transformation

migration to the surrounding austenite. The transport of carbon continues until a high degree of C saturation in austenite is achieved to make it stable both thermally and mechanically. According to some researchers, the process of “pumping” carbon into austenite during the growth of ferrite plates enables achieving carbon concentrations of up to 2.2 wt.% [42, 43]. This transformation stage is characterized by the achievement of an appropriate ferrite-to-austenite content ratio. Depending on the temperature of the transformation, the annealing time and the homogeneity of austenite before isothermal transformation, the resulting microstructure may have a diverse morphology.

5.3.2.3 Kinetics of Isothermal Transformation

In ductile iron, the isothermal transformation occurs in two stages illustrated in Fig. 5.25, which can be written down in the following form:



where:

γ^0 – primary austenite

γ_{HC} – stable (high carbon) austenite

α – lamellar ferrite

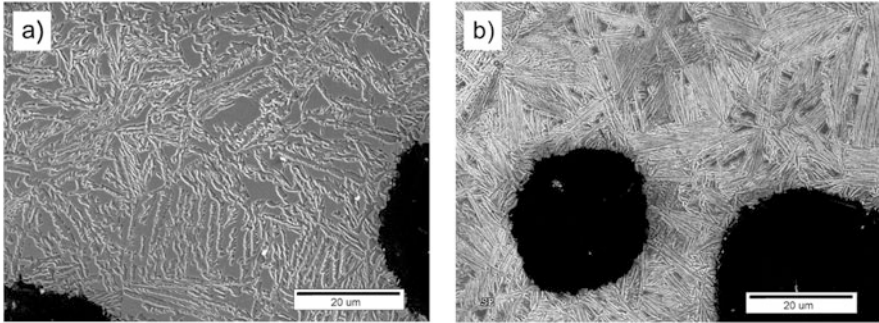


Fig. 5.25 The typical microstructures of austempered ductile iron are shown: (a) temperature of isothermal transformation $T_{it} = 350\text{--}400\text{ }^{\circ}\text{C}$; (b) temperature of isothermal transformation $T_{it} = 260\text{--}350\text{ }^{\circ}\text{C}$ [44]. (Author's own work)

The primary austenite γ^0 with the lowest carbon content is transformed into ferrite plates and high-carbon austenite γ_{HC} . This process begins at the graphite-austenite and austenite-austenite phase boundaries and on the previously formed ferrite plates [44]. During growth of ferrite plates, carbon starts diffusing into the austenite retained in the space between the plates and the process continues until full stabilization is obtained. The end of austenite saturation with carbon to a certain level of concentration and entering the period of the structural stability $\alpha + \gamma_{HC}$ (ausferrite) opens the range of the so-called processing window (t_{i1} to t_{i2}) [44]. Annealing for a time longer than t_{i2} results in the precipitation of carbides, which is the phase undesired in the ADI microstructure. During transformation at a temperature of $350\text{--}400\text{ }^{\circ}\text{C}$, i.e., after the time t_{i2} , the precipitation of ϵ carbide or cementite starts at the α / γ_{HC} interface, leading to the formation of microstructure characteristic of the upper bainite (Fig. 5.25a). Lowering the temperature of austempering reduces the amount of austenite and widens the “processing window” [41]. For this temperature, longer time t_{i2} is associated with the formation of lower bainite with ferrite morphology (Fig. 5.25b), comprising plates with a thickness of several ten to several hundred nanometers. The low temperature of transformation reduces the diffusion rate and prevents carbon transport over long distances, which results in the formation of carbides not only at the α / γ_{HC} phase boundaries, but also inside the ferrite grains.

Studies of various types of cast iron confirm the important effect of chemical composition (especially of alloying additions) and of the austenitizing and austempering temperature on the “processing window” [44, 45]. The research described in [44] shows that increasing the content of alloying additions prolongs the time and reduces the temperature of a stable “processing window.” A similar result is obtained by increasing the austenitizing temperature.

5.3.2.4 Temperature and Time of Austempering

The close dependence of mechanical properties of austempered ductile iron on the parameters of the austempering process determines the choice of temperature and duration of this treatment. Tensile strength and ductility are the most important properties of ADI. Knowing that there is a direct relationship between these properties and the content of different phases in the ADI matrix [46, 47], it is possible to control these properties through control of the content of these phases.

The time/temperature relationship between isothermal transformation and austenite content in the ADI microstructure described by Dymski [48] can be illustrated with appropriate measures of strength or elongation (Fig. 5.26) [48]. The next graph (Fig. 5.27) shows the change of carbon content in austenite depending on the temperature and time of austempering. Increasing the austempering time in the range of 15–240 min results in the increase of austenite saturation with carbon, the increase being most pronounced in the initial period of isothermal transformation. In turn, the highest saturation of austenite with carbon is observed during austempering at 300–350 °C. The degree of this saturation assumes lower values for the temperatures lower and higher than the indicated range. The lower the transformation temperature, the lower is the diffusion rate, the smaller is the size of its products, and the higher is the dislocation density and phase dispersion. All these factors strengthen the heat-treated cast iron.

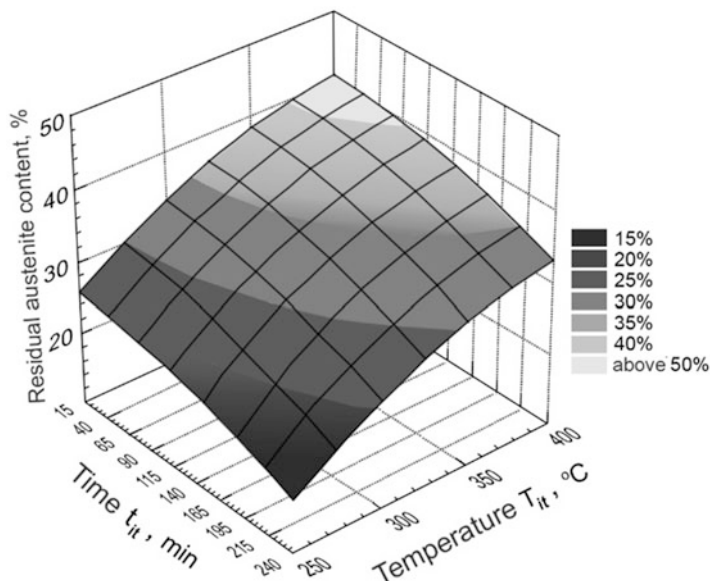


Fig. 5.26 Austenite content (in vol.%) in the ADI matrix as a function of austempering time and temperature. (Based on [48])

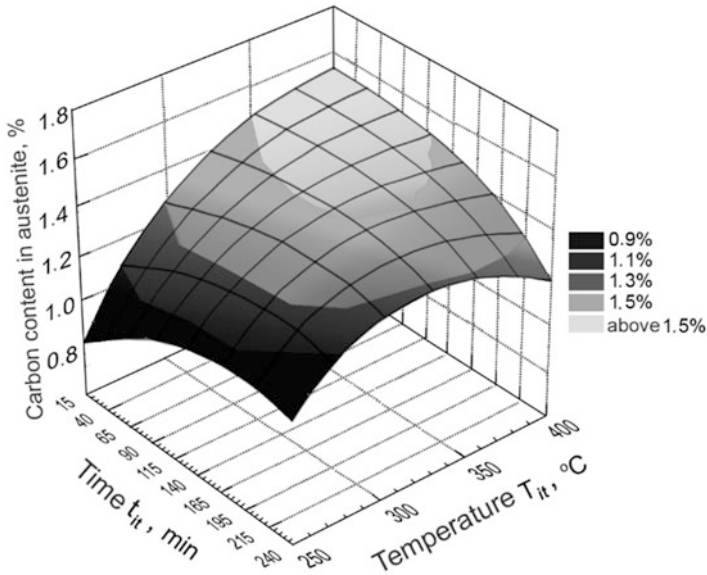


Fig. 5.27 Carbon content (in wt.%) in the ADI matrix as a function of austempering time and temperature. (Based on [48])

And yet, proper selection of the time of austempering may be difficult due to the postcasting chemical composition of the cast iron in microregions. The range of the “processing window” is not always open, which means that the same transformations may not occur simultaneously in the entire volume of the microstructure. At the temperature of the isothermal transformation, there may be permeating areas of austenite still in the process of being saturated with carbon (reaction in Eq. 5.5) and of high-carbon austenite, in which phase II of the transformation has already started (reaction in Eq. 5.6). Differentiation of chemical composition, and especially the content of strongly segregating elements, may be another reason for the modification of “processing window.” The velocity of reactions (Eq. 5.5) and (Eq. 5.6) may be different due to the chemical heterogeneity of eutectic cells and individual phases. Of particular importance here is the uneven distribution of carbon on the cross-section of austenite grains.

5.3.2.5 Mechanical Instability of Austenite

Studies of ausferrite freezing processes indicate that the austenite→martensite transformation at temperatures below M_S occurs only in selected areas of the microstructure, i.e., in the block type austenite (Fig. 5.28). These places are also privileged places for the deformation-induced transformation [19, 49–52]. As a result of this transformation, hard high-carbon martensite is formed. This effect is

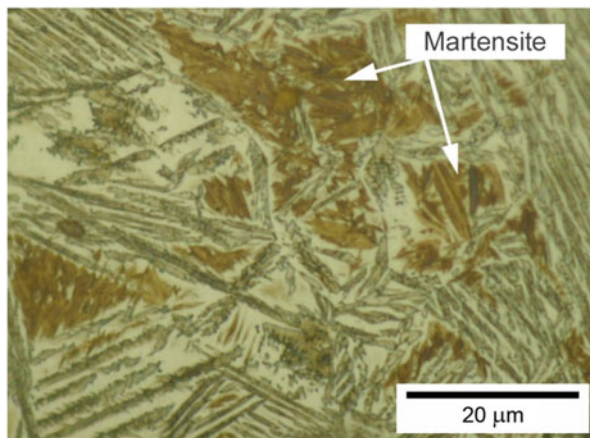


Fig. 5.28 Martensite in the fields of primary block austenite in ausferritic ductile iron. (Author's own work)

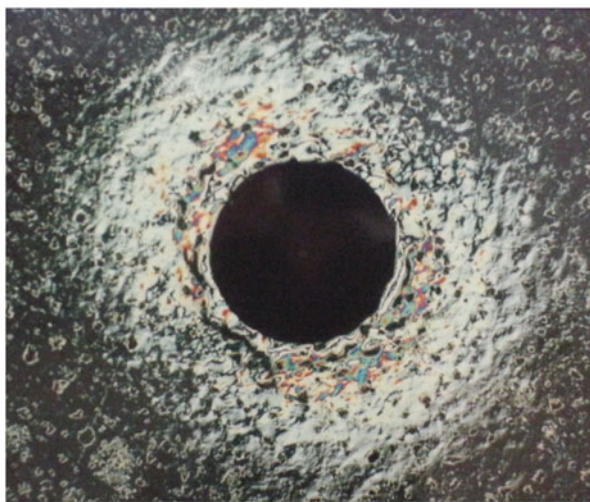


Fig. 5.29 The deformation zone formed on the surface of ausferritic ductile iron as a result of Rockwell hardness measurement; LM, x50, Nomarsky contrast. (Author's own work)

well visible under the microscope in samples subjected to hardness measurements during which the steel indenter permanently deforms the material (Figs. 5.29 and 5.30), creating a zone of plastic deformation around the impression. Martensite formed under the indenter of the hardness tester also creates problems in finding an unambiguous relationship between hardness and austenite content in ausferrite (Fig. 5.31) [33]. The same effect is also observed in other tests, e.g., in static tensile test, resulting in the occurrence of martensite on the fracture of samples which

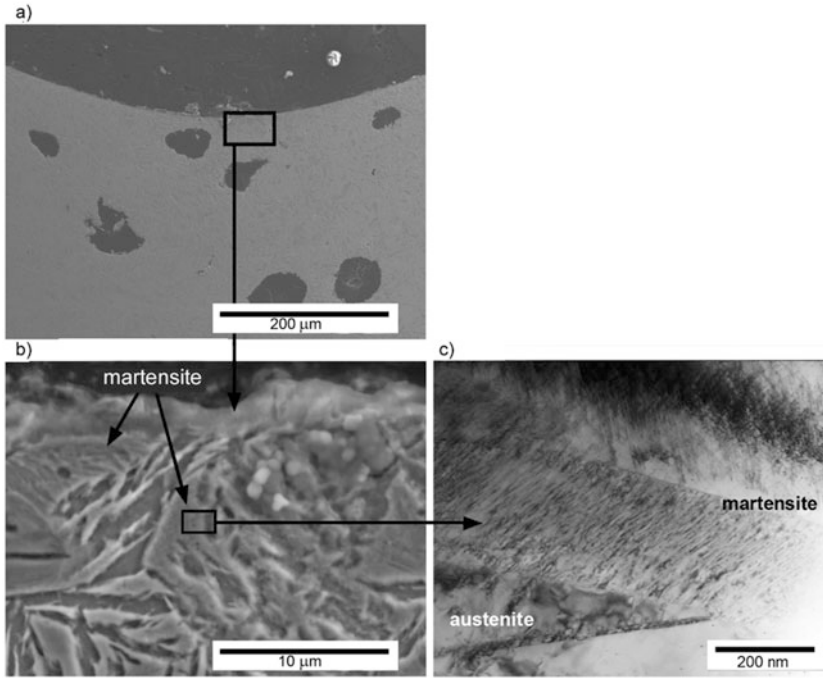
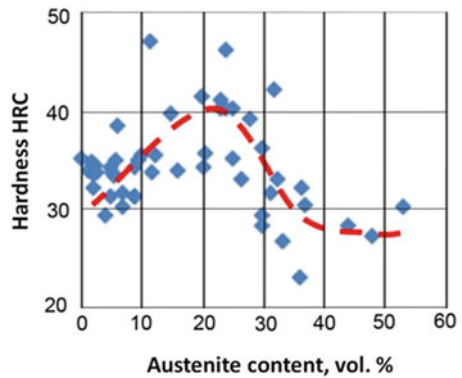


Fig. 5.30 Martensite in the ausferritic matrix of austempered ductile iron after deformation in Brinell hardness measurement: (a), (b) scanning electron microscopy, (c) transmission electron microscopy. (Author’s own work)

Fig. 5.31 Dependence of austenite content in ausferritic ductile iron on its hardness HRC based on the data contained in [20, 21, 29, 32–34, 41, 44–52]



failed during the test [48]. Martensite of this type may also appear during sample preparation and during cutting and abrasion processes [50]. Therefore, based on the transmission electron microscope (TEM) images and X-ray diffractograms, it is difficult to find out whether the examined martensite is a product of transformation induced by the technological process or the result of an incorrect preparation of samples.

The phenomenon described above is related to the problem of obtaining in the material the value of stress or strain which will initiate the transformation of austenite into martensite. This phenomenon occurs in austenite-containing steels and is known as the transformation-induced plasticity (TRIP) effect.

5.3.2.6 Variations of Austempering Treatment

The tendency of austenite with low mechanical stability to deformation-induced transformation is also observed in other technological deformation processes that are not described in this chapter. Investigating the initiation of this transformation by appropriately high stresses and above all plastic deformation, it can be concluded that the transformation can occur in both surface and bulk deformation processes. The analysis of processes occurring in the entire volume of material is more difficult and requires studies of phenomena related to fracture mechanics, allowing for the microstructural heterogeneity of cast iron, casting defects, the presence of graphite, etc., during fatigue or fracture toughness testing. A general statement that can be formulated based on the analysis of the literature and the author's own research is that by minimizing the possibility of the occurrence of TRIP effect, one can obtain an improvement in the "bulk" mechanical properties of ductile iron. Any mitigation of the effect of this phenomenon has its source in the refinement of the ausferritic microstructure and in reducing the content of austenite with low mechanical stability.

As a result of studies of the ausferritic ductile iron, it was found that the value of the strain-hardening exponent n increases linearly with the increasing temperature of austempering. Based on this statement, it has been concluded that n will reach its maximum under the conditions of high austenite content, coarse ferrite, and high temperature of isothermal transformation, while the minimum will fall to the low austenite content and fine ferrite. This is confirmed by the dependence derived by Hayrynen et al., which enables the yield strength to be determined from the size of ferrite plates and the austenite content in matrix [53]:

$$\sigma = AL^{-1/2} + BX_{\gamma} + C \quad (5.7)$$

where:

σ – yield strength

L – size of ferrite plates

X_γ – austenite content

A, B, C – constant values

The dependence shows that it is the size of lamellar ferrite precipitates that controls the value of elastic stress in ausferritic ductile iron. This means that the finer the plates of ferrite in the cast iron matrix, the higher are the strength properties.

Studies on this issue were undertaken and reported in the literature. They were limited to special processes of the heat treatment of ductile iron. The main aim was to refine the microstructure of the cast iron matrix. The refinement was obtained through, higher than in standard processes, undercooling in the first stage of isothermal transformation during two-step austempering (Fig. 5.32) [54, 55] or by conducting low-temperature long-duration thermal processes under special conditions of chemical composition and temperature. These processes of obtaining nanostructural ausferrite is well documented (Fig. 5.33) [56].

It has been reported that compared to the common heat treatment process, undercooling of austenite to a lower temperature of austempering in the first stage of isothermal transformation results in the refinement of ausferrite grains. This reduces the thickness of ferrite plates and thus refines the ausferrite [54]. Also, it has an impact of obtaining slightly higher content of retained austenite compared to the conventional process. The higher retained austenite content and the higher degree of ferrite fragmentation in ausferrite according to relationship in Eq. 5.7 increase the value of the yield strength.

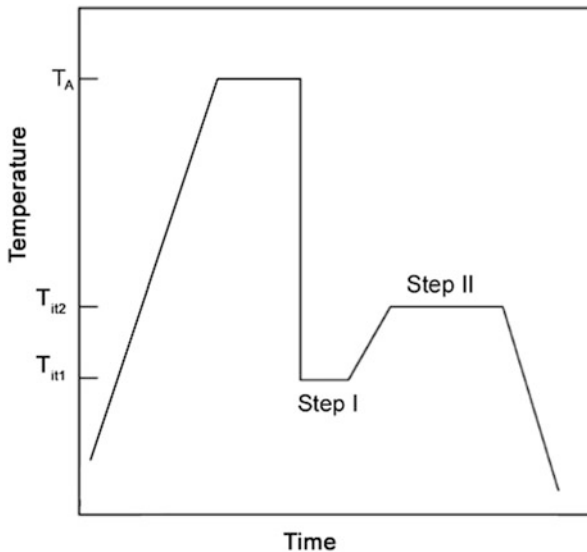


Fig. 5.32 Schematic diagram of a two-step austempering process to obtain ausferritic ductile iron [37]

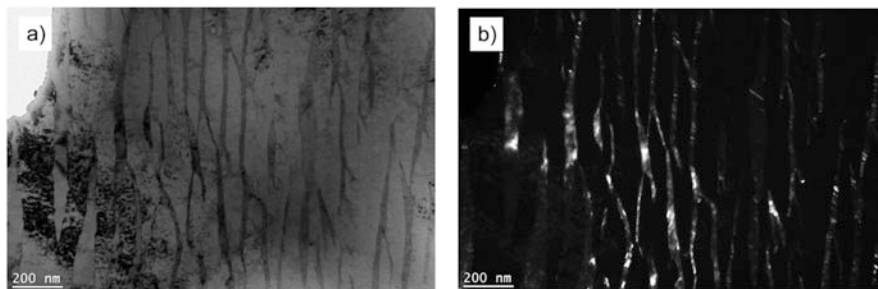


Fig. 5.33 Nanoausferritic structure of ductile iron matrix – a mixture of ferrite and retained austenite plates [56]

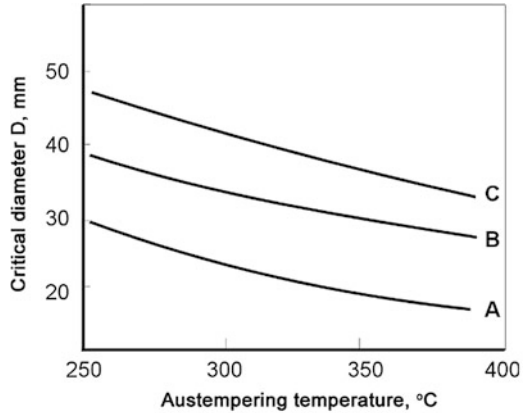
The microstructure obtained in the two-step process reduces the strain hardening exponent n and prevents the achievement of high elongation values (above 11%) in the quasistatic tensile test of cast iron [54]. Hence, it follows that increasing the content of stable retained austenite at the expense of mechanically less stable retained austenite will not be synonymous with improvement of the cast iron plastic properties. It can, therefore, be assumed that it is the mechanism of the deformation-induced martensitic transformation, dependent on the content and stability of retained austenite in the ausferritic microstructure, that is largely responsible for the obtained properties.

5.3.2.7 The Role of Chemical Composition

The choice of cast iron chemical composition to obtain ADI is not always similar to the composition of standard ductile iron grades. The first and one of the most important tasks is to determine the content of basic elements in such a way as to ensure the best possible spheroidization of graphite and the desired type of metal matrix. On the other hand, the quantity of these elements should be such as to counteract the formation of carbides or the tendency to form casting defects. The next task is to control the content of alloying additions, which determines the quality of the microstructure obtained in castings with different wall thicknesses, or to control different cooling rates in casting during austempering.

Austempering of gray nonalloyed cast iron in salt baths is effective only for castings with wall sections thinner than 10 mm (Fig. 5.34) [44]. A slight increase in hardenability occurs when the temperature of the austempering treatment is reduced (up to 30 mm at 250 °C). In the case of using a heating medium other than the salt bath, e.g., a fluidized bed, or in the case of castings with heavy wall sections, obtaining the correct ausferritic microstructure is possible primarily through the introduction of alloying additions [15, 21, 25, 44]. For isothermal transformation, popular and important elements are nickel, copper, and molybdenum added separately or in various combinations.

Fig. 5.34 Influence of austempering temperature on critical diameter for hardenability of ductile iron castings. (Based on [44])



- A Unalloyed ductile iron
- B DI: 0.5wt.%Ni; 0.5wt.%Cu; 3.5wt.%C; 2.2wt.%Si
- C DI: 0.75wt.%Ni; 0.75wt.%Cu; 3.5wt.%C; 2.2wt.%Si

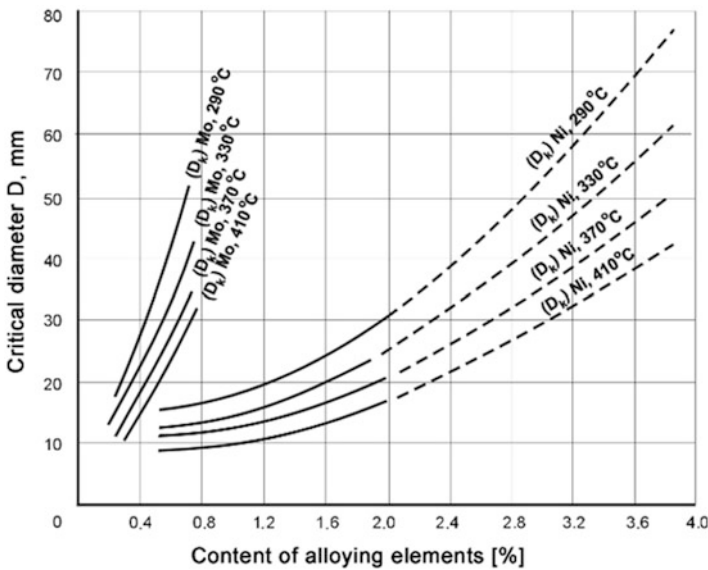


Fig. 5.35 The effect of molybdenum, nickel, and austempering temperature on critical diameter [57]

All the elements mentioned above are introduced primarily to increase the stability of austenite undercooled in the temperature range of pearlite transformation. Introduced together or separately, they increase the hardenability and critical diameter (Fig. 5.35) [57].

The strongest effect on the transformation of undercooled austenite is exerted by molybdenum or its combinations with nickel and copper. The Mo content in ductile

iron is usually limited to ≤ 0.3 wt.% due to its very strong tendency to segregation and formation of $(\text{FeMo})_3\text{C}$ carbides at the boundaries of eutectic cells [32]. Starting with the molybdenum content in cast iron of about 1 wt.% Mo, carbides of the $(\text{FeMo})_3\text{C}_6$ and Mo_2C type can also appear [32].

The composition of ductile iron is usually enriched with 1.5% Cu, up to 4 wt.% Ni and up to 0.3 wt.% Mo. It is assumed that 1.5 wt.% of copper is equivalent to 0.3% Mo. It is, however, recommended to avoid introducing the maximum amount of copper due to its despheroidizing effect [10]. According to Pietrowski [32], copper in ductile iron changes essentially the course of pearlite and bainite transformation. In the temperature range of bainite transformation, copper increases the stability of austenite, slowing down the process of its decomposition.

Nickel added in an amount of up to 1.5% has no significant effect on the increase of austenite stability in the temperature range of pearlite transformation and in an amount of up to 1.0 wt.% in the temperature range of bainite transformation. Copper has similar effect as nickel, and hence cases are known of Ni being replaced with Cu or of both elements co-existing in the cast iron matrix to additionally counteract the formation of molybdenum or manganese carbides [29]. Like copper, nickel reduces the rate of austenite transformation and inhibits its decomposition in Stage II according to reaction in Eq. (5.6). Limitations in the use of Cu and Mo practically make nickel the choice of element that controls the microstructure of ductile iron. There are a few publications [e.g., 32] illustrating the effect of nickel (at a constant content of about Cu and Mo) and wall thickness in ductile iron castings on the microstructure obtained during cooling in the air below 750 °C. This is an example of the possibility of obtaining the ADI microstructure in cast iron of a given chemical composition when cooled in the air or in a casting mold.

5.3.3 *Direct Austempering of Ductile Iron*

“Direct austempering” is a specific process of alloy heat treatment, which consists of a controlled isothermal quenching carried out during casting cooling immediately after its solidification. The process has been studied for over a dozen years in numerous research and development centers for various types of foundry materials [42, 43, 58–60].

Increasing the cooling rate of casting from the solidus temperature, done by knocking out the casting from mold and cooling it down in the air or quick cooling to a predetermined temperature, is a well-known method of controlling the metal microstructure. This procedure is usually applied to aluminum alloys to simplify the heat treatment cycle and increase the hardness of the parts obtained. The solution heat treatment of aluminum alloys directly after casting is to some extent similar to the direct hardening of iron alloys. In this case, rapid cooling (e.g., in water) of an aluminum casting with a temperature below the solidus line is used immediately after removal from the casting mold (metal mold in this case). In contrast to austempering, this type of a fast cooling of Al alloys leads to a saturation of the

casting with alloying constituents which, during later aging, gives rise to the effect of precipitation hardening. This process is slightly different in the case of direct austempering.

It is a well-known fact that when the cast iron cools down from the temperature of 1130–1150 °C, the casting “passes” through a temperature range of 950–815 °C, which is the range used for the austenitizing process during conventional heat treatment of ADI. So it seems logical to remove the hot casting from the mold in this temperature range and subject it to rapid cooling to a temperature at which it will be austempered. In this way it is possible to avoid cooling of casting and reheating it to the austenitizing temperature (Fig. 5.36).

It should be emphasized how important and beneficial this simplified heat treatment is. It is an indisputable fact that in addition to the appropriate properties, the attractiveness of the product also depends on its price. In the case of ADI, the cost calculation depends on several fixed factors at individual stages of the technological process. Heat treatment of ductile iron is still a very expensive element of the whole technological process. Therefore, its simplification, e.g., through the use of direct austempering, leads to significant savings, which are composed of a number of factors:

- Significant savings of electricity, which would have to be used to reheat the castings to the austenitizing temperature, and consequently reduced volume of raw materials necessary to produce such energy, less harm to the natural environment and lower environmental pollution associated with electricity generation in conventional power plants
- Elimination of additional equipment for high-temperature heat treatment, which is very important for production plants with limited resources of specialized equipment and funds for their purchase

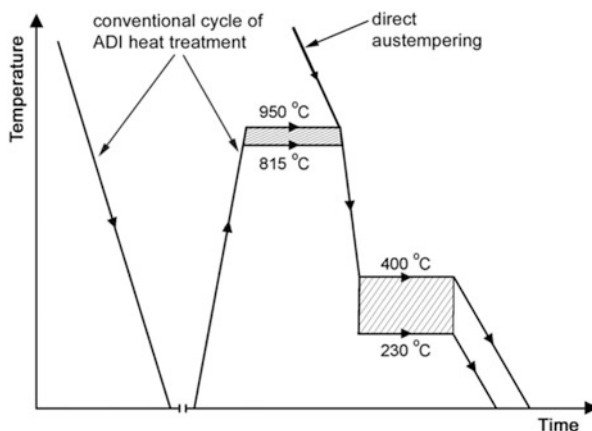


Fig. 5.36 Comparison of the conventional heat treatment cycle and direct austempering of ADI. (Author’s own work based on [26, 61–63])

- Saving space, which would be occupied by devices for the austenitizing treatment
- Significant time saving of product manufacture, which should be expected especially in large-lot orders

Clearly defined benefits resulting from direct austempering are not, however, equivalent to obtaining the construction material with the desired in-service mechanical properties. Detailed analysis of the phenomena which occur during cooling and subsequent heat treatment and of the processes that occur during direct austempering suggests the possibility of some structural differences that may be reflected later in the properties of ADI castings. Although it is difficult to determine which of them and in what way (positive or negative) will affect the in-service mechanical properties of castings, from a production point of view this technology seems very interesting.

Owing to the research made in various scientific centers around the world, several ways of conducting the direct austempering process of ductile iron castings are known, to mention the use of metal molds, sand molds and the full mold process. The experience gained during their implementation allows describing the transformations and phenomena that accompany the ductile iron direct heat treatment process.

5.3.3.1 Microstructure and Properties

The description of the direct austempered ductile iron (DADI) microstructure should start with the statement that this microstructure is shaped in a different way than the microstructure of conventional ADI cast iron. The main reason is the lack of typical austenitizing treatment, i.e., absence in the direct cycle of the eutectoid $\gamma \leftrightarrow \alpha + \text{Fe}_3\text{C}$ transformation. The microstructure of DADI rather retains its original character, which means that it consists of austenite dendrites and eutectic cells on a microscale and of “macrocells” on a macroscale [26, 61]. Isothermal transformation does not exert a great influence on the structure modification, and, therefore, the primary microstructure should be expected after the casting has cooled down to ambient temperature (Fig. 5.9). The result may be greater heterogeneity in the chemical composition of ductile iron matrix, larger dimensions of products of the isothermal transformation, and directional character of the microstructure.

Rapid cooling of the casting from the temperature below the solidus line results in a specific “freezing” of the DADI primary microstructure, preventing the diffusion of its constituents, carbon in particular, at the temperature of the austenitizing treatment and lower temperature. This phenomenon results in greater homogeneity of the matrix in the vicinity of graphite precipitates than in the case of the usual cooling of cast iron during which the graphite nodules grow at the expense of carbon present in the surrounding matrix. The austenitizing treatment used in the conventional cycle makes the cast iron matrix homogeneous by redistribution of carbon, including partial dissolution of graphite nodules [32]. During the direct heat treatment of ductile iron, this effect will not occur. It should

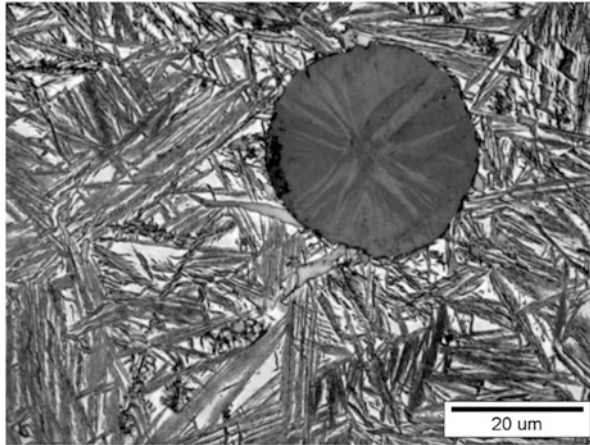


Fig. 5.37 Microstructure of DADI cast iron (austempering temperature = 300 °C, time = 90 min.). (Author's own work)

be noted that in the case of DADI, there is also absence of carbon diffusion toward the graphite nodules during slow cooling of the casting from the solidus temperature to ambient temperature. This leads to a “bull eyes” structure. It can, therefore, be assumed that in DADI the concentration of carbon in the vicinity of graphite precipitates should be comparable to ADI or even higher. Images of the microstructure of samples taken from DADI under identical conditions with ADI (austempering temperature = 300 °C, time = 90 min.), shown in Figs. 5.37, confirm these assumptions. It follows that in the case of conventional treatment, the transformation rate near the graphite/austenite interface must be high since products of this transformation show a high degree of refinement. The high rate of austenite transformation into ferrite suggests a lower carbon content in the microregions or higher silicon content allowing for the occurrence of this kinetics. Hence it follows that the extent of homogenization of the DADI matrix can be equal to that of ADI or possibly even higher.

The phenomena that occur at the boundaries of eutectic cells or dendrites may assume the course slightly different than in the case described above. Austenitization of ductile iron, carried out during conventional heat treatment aimed at obtaining ADI, may lead to a redistribution of elements grouped in these microregions. This phenomenon does not occur during direct austempering, and hence the conclusion follows that the DADI matrix will be more heterogeneous in the areas of the austenite/austenite phase boundaries. Additionally, austenitizing treatment enables dissolution of the undesired phases appearing in ductile iron, e.g. carbides. The lack of austenitizing treatment during direct austempering does not create conditions for the dissolution of carbides that may have appeared during solidification.

Analysis of individual constituents occurring in the DADI microstructure is in practice reduced to the basic phases present in the matrix, i.e., ferrite and austenite.

However, some irregularities have been found, which also suggest the need to investigate the characteristics of the precipitates of nodular graphite.

As in the case of all other types of ductile iron, nodular graphite is one of the most important constituents of the DADI microstructure. During the process of direct austempering, some differences in the formation of this phase were noted compared to the standard types of ductile iron, including ADI. The reason is that the direct heat treatment inhibits the growth of graphite nodules in the solid phase, which runs all the time during cooling of the casting, although at a constantly decreasing speed. As mentioned earlier, in the case of DADI, a specific “freezing” of the microstructure occurs, thereby inhibiting the diffusion of carbon into the graphite nodules as soon as the intensive cooling to the temperature of the austempering treatment starts. The above leads to the formation of graphite nodules characterized by a smaller volume and to milder heterogeneity of carbon distribution in the matrix surrounding the graphite and to less deformation. This is consistent with the studies presented in [62] and systematic measurements of the size of graphite particles present in the microstructure of castings made from DADI and ADI originating from the same melts. The results indicate that the average diameter of graphite nodules is approx. 31 μm in DADI, while in ADI this value is at a level of 35 μm , which means that it is by about 10% higher than in DADI.

Ferrite, present in DADI in the form of plates, is slightly different from the ferrite formed in the ADI matrix. It was found earlier that these plates are characterized by a specific orientation and form structures coarser than in ADI. The plates are longer during direct austempering at a lower temperature, but their length decreases when austempered at high temperature. Changes also occur in the shape and thickness of plates (Figs. 5.38 and 5.39). Lower austempering temperature affects the shape of the plates in such a way that they become more “sharp-pointed,” resembling

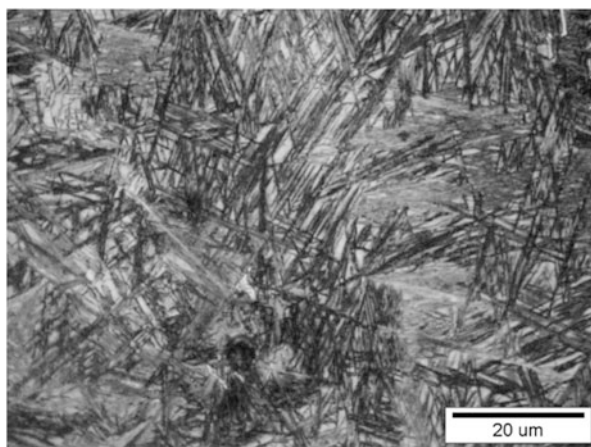


Fig. 5.38 Fine lamellar ferrite in the matrix of DADI (austempering temperature = 260 °C, time = 90 min.). (Author’s own work)

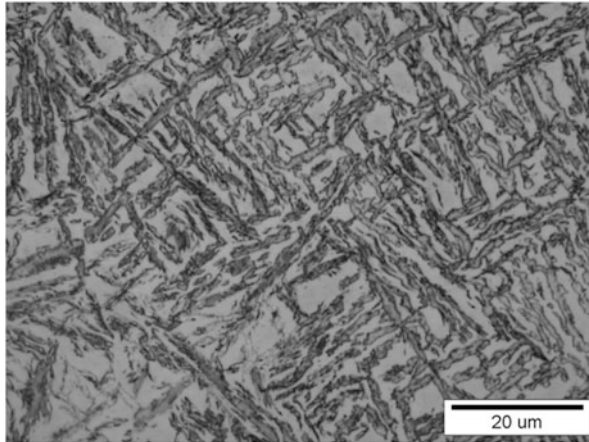


Fig. 5.39 Plates of “feathery” ferrite in the matrix of DADI (austempering temperature = 360 °C, time = 90 min.). (Author’s own work)

martensite in their appearance, and have also smaller thickness of approx. 0.2–0.8 μm . Higher temperature of direct austempering makes the plates more ramified. They look more “feathery” and the thickness grows to approx. 1.2 μm .

Retained austenite present in the DADI matrix has also been examined in relation to the austenite found in ADI. The most important conclusion that followed this analysis is that under the same conditions of the austempering treatment, the proportional content of austenite in the microstructure of DADI is slightly higher than in ADI. Proper amount of retained austenite is usually associated with the ADI plasticity. Its presence in DADI is confirmed by a SEM image of the fracture showing numerous dimples (Fig. 5.40) [63]. The DADI matrix is mainly composed of the lamellar ferrite and retained austenite. As demonstrated by the microanalysis and TEM examinations, the matrix may also contain carbides and martensite, which are phases undesirable in the microstructure of both DADI and ADI.

The presentation of DADI mechanical properties should start with the statement that only in a very few cases of direct heat treatment, attempts to achieve the strength/ductility combination consistent with the requirements of the European Standard EN 1564 for ADI have ended in success. This fact is graphically presented in Fig. 5.41. In spite of this, the results obtained for DADI indicate that its properties far outweigh those guaranteed by other types of “ordinary” ductile iron. It is interesting to compare the properties of DADI and ADI obtained for the same conditions of the austempering treatment.

The information presented in the previous subsections reveals some basic facts concerning DADI cast iron, which would be worth emphasizing. Ausferrite in the DADI matrix differs slightly from the ausferrite obtained by conventional austenitizing and austempering. For the same heat treatment parameters, in the DADI matrix a higher content of the stable retained austenite was recorded,

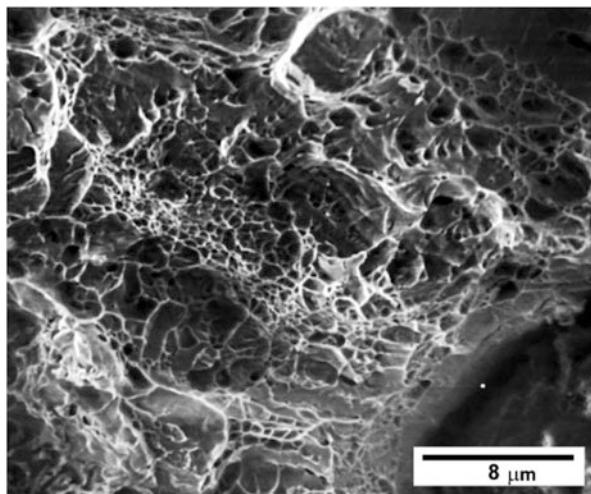


Fig. 5.40 DADI. SEM fractograph showing dimples characteristic of ductile fracture. (Author's own work based on [63])

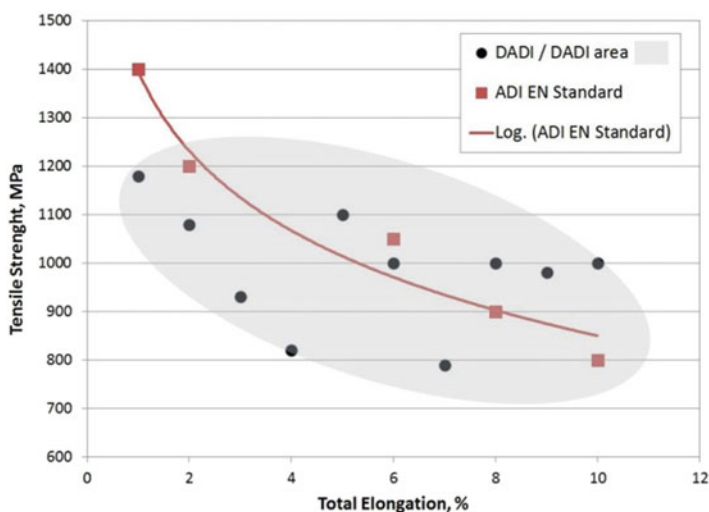


Fig. 5.41 Mechanical properties of DADI compared to the properties of ADI included in the EN 1564 Standard. (Author's own work)

accompanied by the ferrite strongly saturated with carbon. Compared to ADI, the microstructure of DADI seems to be coarser. Additionally, in DADI, some areas with increased concentration of alloying additions have been identified, especially at sites referred to as last to freeze (LTF), which were not found in the structure of ADI. Molybdenum occurring in LTF microregions can contribute to the formation

of Mo_xC_y carbides (identified in the research presented in [47]), the presence of which increases DADI hardness but significantly deteriorates its plastic properties.

Based on the analysis of the thermal history of castings subjected to the direct austempering and conventional austempering, it was found that the contribution of various mechanisms of hardening the DADI matrix is slightly different than in the ADI cast iron. Closer analysis of the hardenability of both types of cast iron suggests that the most important factor responsible for the lower ductility and fracture toughness of DADI compared to ADI is a coarse metal matrix, left unrefined due to the omission of the $\gamma \leftrightarrow \alpha + \text{Fe}_3\text{C}$ eutectoid transformation, which occurs during cooling of the casting and its reheating for the austenitizing treatment. The explanation for the high yield strength $R_{0.2}$ of DADI, similar to the values obtained in ADI, should be sought in the strain hardening effect resulting from the higher density of dislocations in austenite and ferrite and from the presence of microtwins. However, the main reason for the high DADI strength is, as in ADI, the solid solution strengthening of both ferrite and austenite. Saturation of both phases with carbon is the reason for DADI in the considered variants of austempering treatment to reach a tensile strength, R_m , of 1200 MPa.

The above statements characterizing the ductile iron obtained as a result of direct heat treatment are sufficient to conclude that DADI has the mechanical properties slightly inferior to ADI. It was also noticed that extending the time of DADI austempering has increased both strength and elongation. DADI is competitive with ADI not only in terms of higher mechanical properties, hardness in particular, but also in terms of the production cost. A brief analysis of the production process shows that the cost of producing a DADI blade for the shot blasting machine is by 9% lower than in the case of ADI and by 25% lower than in the case of alloyed high-chromium cast iron with the addition of molybdenum, so far the standard material for this product [62].

5.3.4 Ausforming

The refinement of ausferrite grains in the matrix of gray cast iron can also be obtained by combined plastic forming and heat treatment, generally known under the name of ausforming. This is a very interesting issue and since it has recently gained wide recognition among scientists, special attention will be paid to this type of cast iron.

Hot or cold plastic forming of cast materials refines their structure, reducing shrinkage and gas porosity and microsegregation of alloying elements. It also provides additional nucleation sites during austenite transformation after deformation or recrystallization. These assumptions were adopted in the high-temperature deformation process before the start of austenite transformation in a ductile iron matrix. Studies show that ausforming during ausferritic structure formation significantly shortens the time necessary to trigger the austenite-ferrite transformation by introducing additional energy into the system through mechanical action [64].

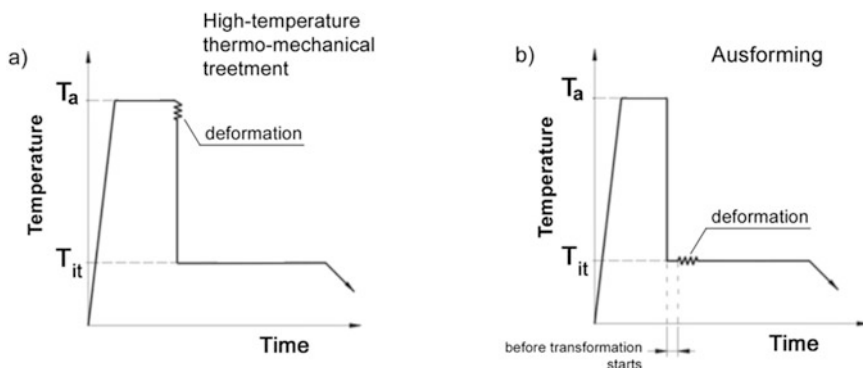


Fig. 5.42 Thermal processing of ductile iron: (a) high-temperature thermo-mechanical treatment, (b) ausforming. T_a and T_{it} are temperatures of austenitization and isothermal transformation, respectively. (Based on [65, 66])

It was also found that austenite saturation with carbon was higher than in the conventional process, which also indicates an acceleration of the reaction. The increased ferrite nucleation rate leads to fragmentation of the ausferritic structure and ensures better homogeneity of the alloy, and hence also of its component phases [65, 66]. A more homogeneous structure prevents the occurrence of martensite at ambient temperature even after a short bainite transformation time.

Processes completed with 25% deformation show that cast iron dramatically gains in mechanical properties. At least 70% increase in the yield strength and 50% increase in the tensile strength as compared to the conventional ADI were demonstrated. However, depending on the temperature and mode in which the process of deformation is carried out, castings will change their properties. For the thermoplastic treatment shown in Fig. 5.42, alloyed cast iron characterized by high hardenability often with the additions of Ni and Mo should be used. Alloying additions are also important when ausforming is carried out on products with large cross-sections and when high degrees of the deformation are applied. Ausforming carried out on nonalloyed cast iron was found to significantly reduce plasticity with only a minimum increase in strength.

For simple products, methods of forging gray iron castings have been proposed. Special preforms would be used for this purpose from which the casting would be transported to a bath ensuring thermal treatments in the temperature range of bainite transformation [64].

5.4 Mechanical Properties

The richness of the variants of cast iron structure provides this material with an extremely wide range of achievable properties. Not all of them can be discussed here, but, apart from the most important ones which include comparable strength to steels, good fracture toughness, and high abrasion resistance, it is worth paying

attention to the properties less often discussed, e.g., corrosion resistance, good thermal conductivity, and resistance to the effect of low or high temperature [14, 17].

5.4.1 Strength of Cast Iron

The strength of gray cast iron is primarily a function of its structure, where the type of matrix and the content, shape, and distribution of graphite precipitates are of importance [14, 17]. In general, increasing the amount of pearlite in the matrix increases the value of R_m and reduces the plasticity, which results from the mechanical properties of pearlite and ferrite (pearlite: $R_m = 550\text{--}850$ MPa, medium plasticity: $A_5 = 2\div 10\%$, ferrite: $R_m = 350\text{--}500$ MPa, high plasticity: $A_5 = 10\div 22\%$). In gray cast iron with flake graphite, increasing the amount of pearlite in the matrix from 70 to 100 vol.% increases the value of the tensile strength R_m by 20–35 MPa. The low strength of cast iron with a martensitic matrix is caused by the presence of quenching stresses.

A similar relationship governs the type of ductile iron matrix and its strength. In this type of cast iron, ferrite formation leads to a reduction in the tensile strength R_m and improvement of plastic properties (Fig. 5.43) [14]. Increasing the proportion of pearlite in white cast iron (with simultaneous reduction in the content of cementite) increases not only the tensile strength, but also the ductility of white cast iron.

The parameters of the cast iron primary crystallization also exert a significant effect on the strength of this material. The tensile strength of cast iron increases with the increasing content of the dendrites of primary austenite, with the increasing degree of their branching and with the increasing number of eutectic grains (Fig. 5.44) [14].

The strength and ductility of metal matrix decrease to a large extent due to the presence of graphite precipitates in the cast iron structure. The negative influence of graphite results from the reduction of the active cross-section of the metal matrix and also from the fact that in this matrix graphite particles play the role of micronotches. With the same total volume of graphite in cast iron, the reduction of the active cross-section is the least severe in the cast iron with nodular graphite, and the most severe in the cast iron with flake graphite. For graphite flakes with elongated shapes, the degree of reduction of the active surface can reach even 50%, especially when casting walls have small cross-sections. The fact that graphite particles act as micronotches in the cast iron matrix is due to the shape of these precipitates. This effect is weakest in the nodular graphite and strongest in the graphite in the shape of sharp-ending flakes.

Summing up, it can be stated that in gray cast iron with the decreasing content of graphite precipitates and the increasing degree of their refinement, both cast iron strength and ductility tend to increase. The transition from the flake graphite to the nodular graphite significantly improves the strength and even more the ductility of the cast iron.

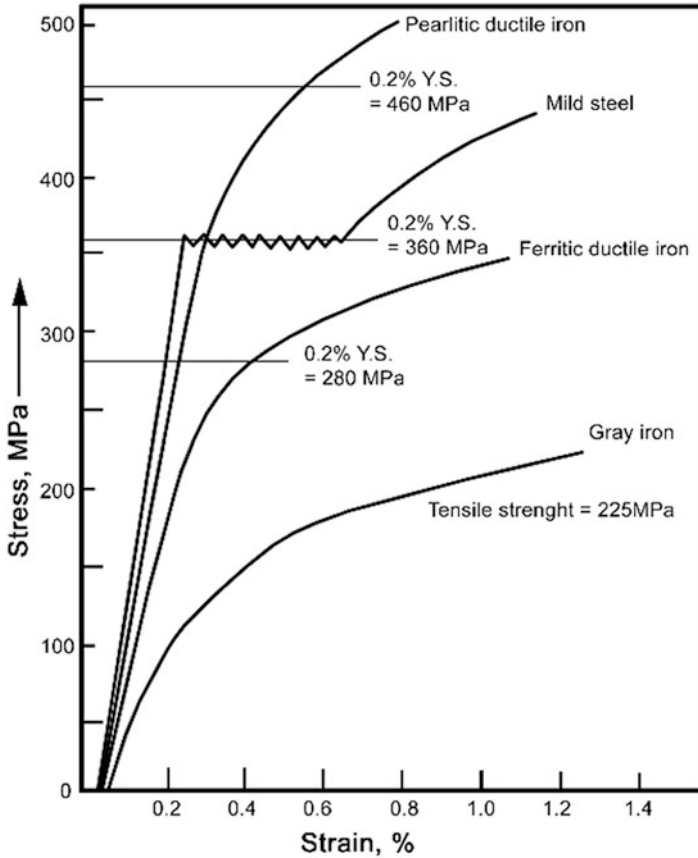


Fig. 5.43 Curves illustrating the elastic and plastic behavior of mild steel, cast iron with flake graphite, and cast iron with nodular graphite with a ferritic and pearlitic matrix. (Based on [14])

Figure 5.45 shows the effect of the content of regular nodular graphite on the tensile strength of ductile iron with different types of matrix [14]. The harmful effect of the presence of various forms of graphite is best visible in the case of purely pearlitic matrix. However, an ausferritic matrix, obtained as a result of heat treatment, mainly of ductile iron, has the strongest influence on the cast iron strength.

The advantage of ductile iron with ausferritic matrix is primarily a unique combination of mechanical properties (Fig. 5.46) [15–18]. The high temperature of austempering treatment (reaching 400 °C) enables producing the cast iron characterized by high elongation and tensile strength at a level of 850 MPa. At a relatively low transformation temperature, e.g. 260 °C, ADI grades with strengths of up to 1600 MPa are obtained. They are additionally characterized by a very high hardness and excellent abrasive wear resistance.

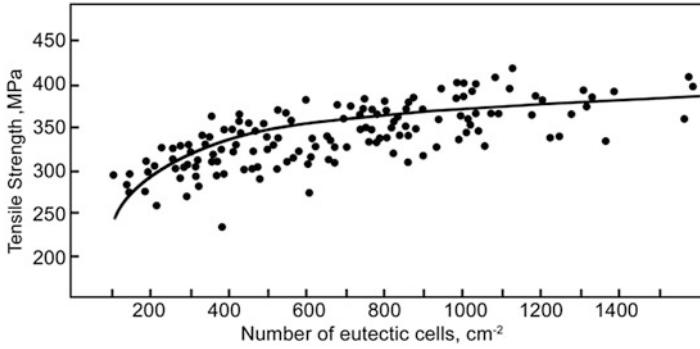


Fig. 5.44 Influence of the number of eutectic grains on the tensile strength of nonalloyed gray cast iron with flake graphite. (Based on [14])

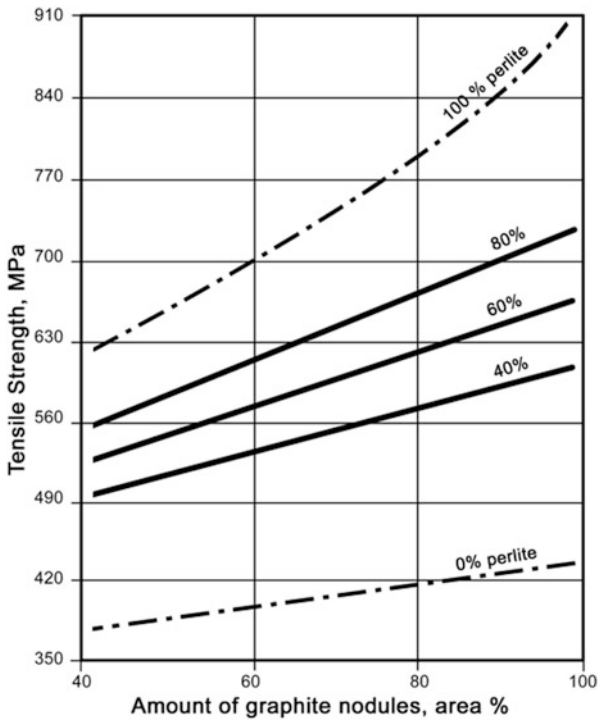


Fig. 5.45 Influence of the content of nodular graphite (lower than 100% content of the nodular graphite means its degeneration toward the vermicular or flake form) and pearlite on tensile strength. (Based on [14])

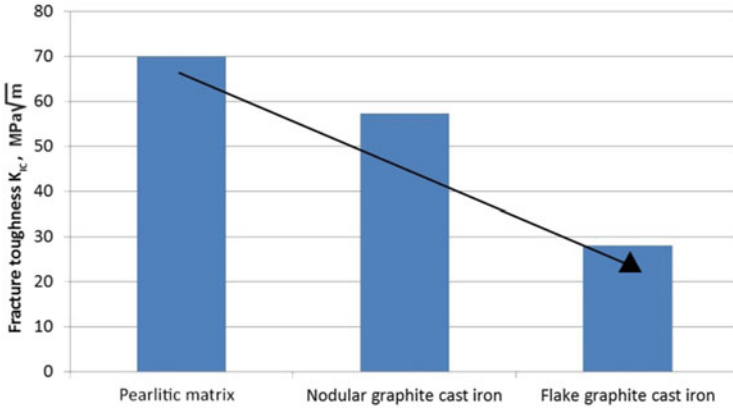


Fig. 5.46 Influence of graphite form on the fracture toughness (K_{1C} value) for eutectic cast iron with pearlitic matrix. (Author’s own analysis based on [14, 17])

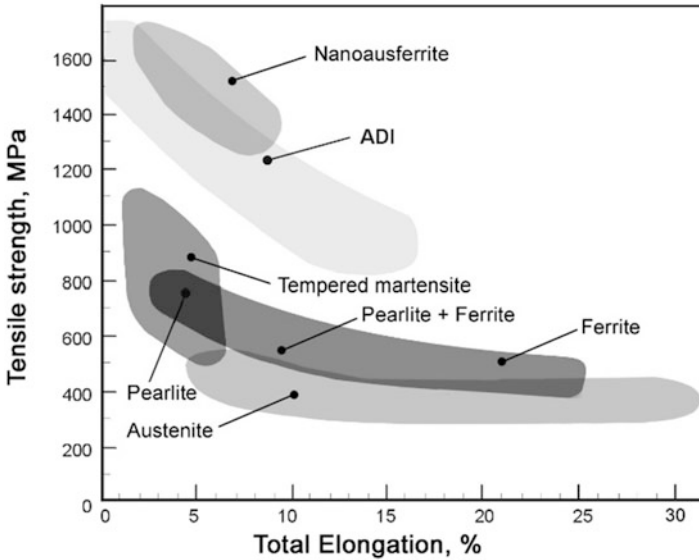


Fig. 5.47 Mechanical properties of ductile iron with various types of matrix. (Author’s own analysis based on [15–18])

5.4.2 Fracture Toughness

The effect of primary structure, and especially of graphite precipitates present in this structure, on the cast iron tendency to cracking is quite significant [24]. The presence of graphite precipitates acting as micronotches drastically reduces the value of fracture toughness (K_{1C}) as shown in Fig. 5.47. for the eutectic cast iron with

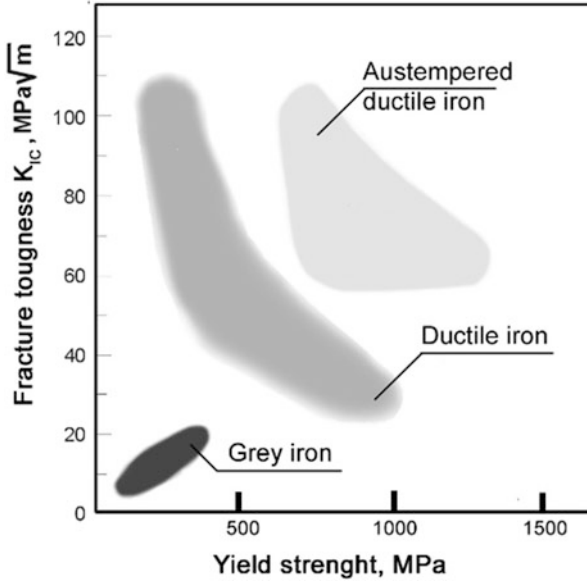


Fig. 5.48 Different types of ductile iron compared in terms of their fracture toughness (K_{IC} value). (Author's own analysis based on [14, 17, 33])

flake graphite and with nodular graphite compared to a purely pearlitic matrix [14, 17]. The most important factors that control the gray cast iron fracture toughness include the shape and dispersion of graphite precipitates and absence of carbides, nonmetallic inclusions and porosity.

Assuming that the spherical shape of graphite is the optimal one, it can be concluded that fracture toughness depends to a large extent on the type of cast iron matrix. The drawing shows the relationship between fracture toughness and various types of ductile iron matrix after heat treatment. The graph in Fig. 5.48 [14, 17, 33] indicates that the ADI grades with the highest strength have better fracture toughness than the ductile iron based on a pearlitic matrix or matrix of tempered martensite. On the other hand, compared to pearlitic ductile iron, the ADI of a lower strength has an almost double K_{IC} value. All tests in which ADI shows fracture toughness better than or comparable to other materials (e.g. ductile iron, forged steel or carburized steel) emphasize one fact, namely that along with the increase in austempering temperature, the resistance to impact loads also increases, reaching a maximum at 340–370 °C (Fig. 5.49) [17, 33]. This characteristic is a direct proof of the relationship between fracture toughness and austenite content in the ADI microstructure.

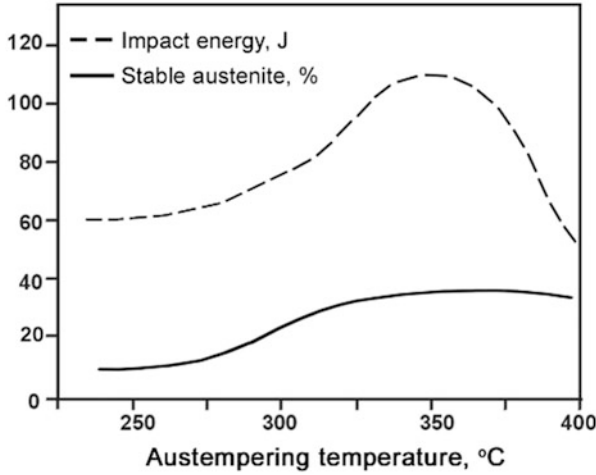


Fig. 5.49 Relationship between stabilized austenite content in ADI microstructure and elongation and impact toughness. (Author’s own analysis based on [17, 33])

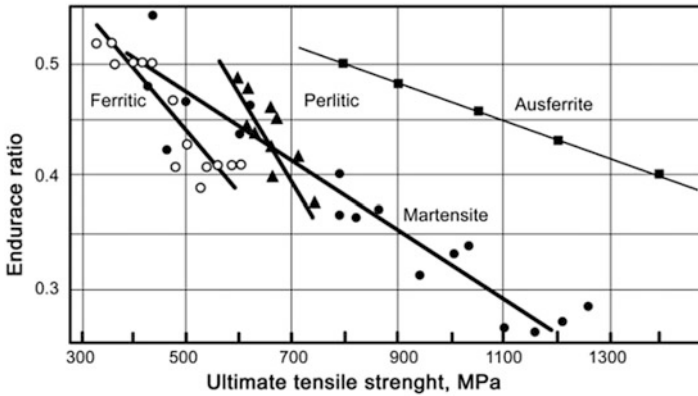


Fig. 5.50 Fatigue strength to tensile strength ratio (endurance ratio) for ductile cast iron. (Author’s own analysis based on [14, 17, 25])

5.4.3 Fatigue

The structure of cast iron affects its fatigue strength primarily through the shape and size of graphite particles. Therefore the ratio of fatigue strength to tensile strength decreases from a value of about 0.5 for the fine precipitates of flake graphite to a value of about 0.3 for the cast iron with nodular graphite. Hence it follows that the change of graphite shape from flakes to nodules affects to a lesser extent the increase in fatigue strength than the corresponding increase in tensile strength (Fig. 5.50) [14, 17, 25]. The fatigue strength of cast iron decreases with the increasing size of graphite flakes.

In the case of fatigue strength, the impact of the matrix is not as spectacular as in the case of fracture toughness, but even then, it is worth paying attention to one characteristic feature of the cast iron after heat treatment. It is the possibility to mechanically harden the surface of finished ADI castings by burnishing, shot blasting or machining. This is due to the presence of carbon-saturated austenite in the deformed microstructure. Machining triggers the mechanism of the deformation-induced austenite transformation into martensite. This mechanism combined with the deformation by twinning causes additional hardening of the casting surface [52, 67]. Literature data suggest that, due to this effect, some ADI grades are in this respect comparable to or better than forged steels [14, 17].

As in the case of fracture toughness, also for fatigue strength, a relationship can be derived between this property and the heat treatment parameters or, in other words, between the content of unreacted austenite in ADI and mechanical properties of this cast iron. This is illustrated by the graph in Fig. 5.50 showing the fatigue strength-to-tensile strength ratio of ADI. For cast iron grades with lower strength, this ratio reaches 0.5 and decreases below 0.3 with an increase in tensile strength R_m .

Comparison of fatigue strength of various materials, including two classes of ADI cast iron, provides interesting information concerning the use of this material for gears [17]. From the presented results of studies it follows that surface hardening of castings made from ADI significantly increases their fatigue strength, which is higher than in the common and conventionally hardened ductile iron and cast steel grades, and is comparable to steel subjected to surface hardening treatment [24, 50–52].

5.4.4 *Wear Resistance*

Though abrasive wear of cast iron mainly depends on the conditions under which the wear process occurs, the structure of this material and the properties of its individual constituents also exert an important effect on the wear intensity (Table 5.3) [14, 16, 17, 19, 25, 33, 68]. Abrasive wear is usually directly related to the hardness of the material and the ratio of the cast alloy to abrasive material hardness values. Therefore, to improve the abrasion resistance of cast iron, alloying elements forming hard phases are introduced.

The material of the highest abrasion resistance under the conditions of low dynamic loads is white cast iron containing cementite [14, 17]. The chemical composition of this material is determined taking into account the carried load and the temperature at which it performs. At high load values, it is advantageous to reduce carbon and phosphorus content in spite of the related drop in hardness. Abrasion resistance of the white cast iron is observed to increase with the increasing proportional content and dispersion of cementite. In both white and gray cast irons, this property decreases with the increasing interlamellar spacing of pearlite. Wear

Table 5.3 Comparison of hardness values of cast iron structural constituents. (Based on [14, 16, 17, 19, 25, 33, 68])

Structural constituent of cast iron	Hardness HV
Unalloyed ferrite	70–200
Unalloyed austenite	170–230
Alloyed austenite	250–600
Unalloyed pearlite	250–320
Alloyed pearlite	300–460
Ausferrite	280–550
Martensite	500–1010
Cementite	840–1100
$(Cr,Fe)_7C_3$	1200–1600

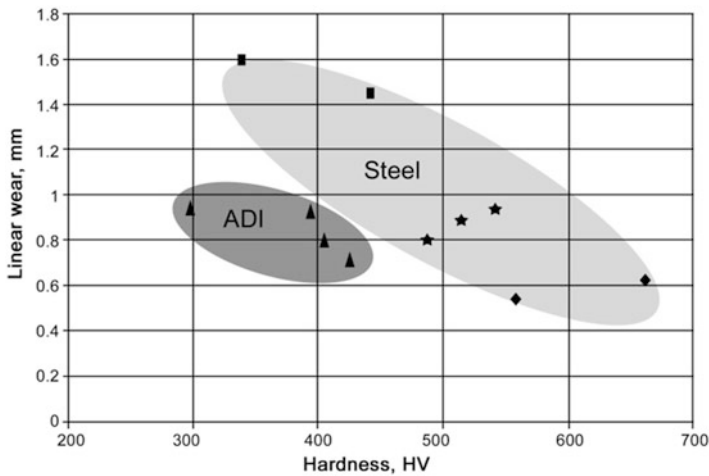


Fig. 5.51 Abrasive wear resistance compared for different materials. (Author's own analysis based on [67–69])

resistance increases with the matrix changing from pearlitic through ausferritic to martensitic.

So far, for the cast iron with an ausferritic matrix, a definite relationship between hardness and wear resistance has not been found (Fig. 5.51) [68, 69]. It turns out that slightly lower hardness of ausferritic cast iron does not prevent it from competing with steel with a hardness of 600 HV. This is due to the aforementioned surface hardenability of ADI where through mechanical action the critical stresses are overcome causing deformation-induced martensitic transformation and strain hardening by twinning. The result of this surface hardening is definite increase in hardness (Fig. 5.52). Both the surface hardening effect and the special microstructure of ADI translate into better wear resistance.

An interesting case is the new type of cast iron proposed by American scientists called carbide austempered ductile iron (CADI) [70]. This material combines the features of ADI with the structure of cast iron containing hard chromium carbides

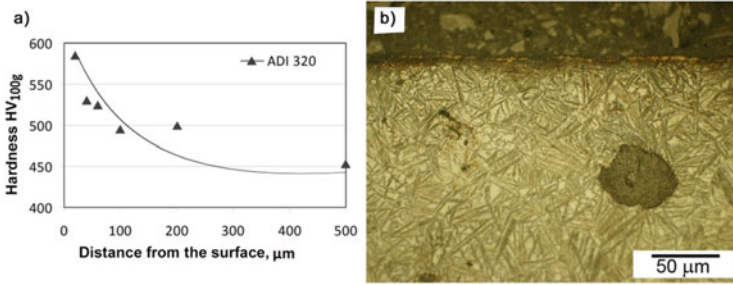


Fig. 5.52 (a) Hardness distribution in the surface layer and microstructure of ausferritic ductile iron (ADI 320 grade) after abrasion process carried out with loose abrasive medium, (b) typical microstructure after abrasion. (Author's own work)

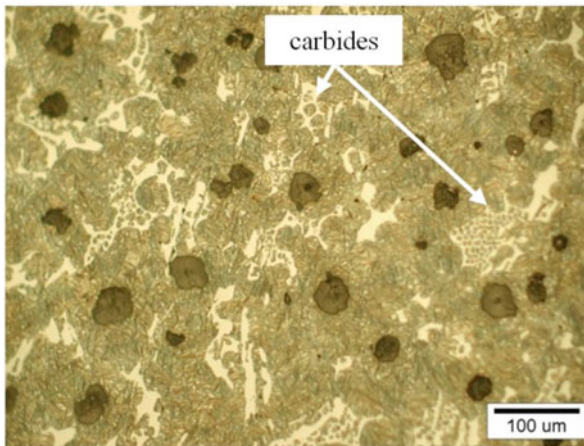


Fig. 5.53 Microstructure of carbidic austempered ductile iron (CADI). (Author's own work)

in a proportion of up to 18 vol.% (Fig. 5.53). This structure, by providing adequate strength to cast iron, enables 40% improvement in wear resistance compared to the common ADI grades [70].

5.5 Applications and Future Perspectives

Cast irons are the most popular foundry materials, also constituting the largest tonnage share. They account for 70% of world production of castings (Fig. 5.54), which is mainly due to the variety of properties offered by castings. Comparable proportions of individual foundry materials are found in all countries in which the foundry industry is highly developed (Fig. 5.50) [13] despite the growing demand for light alloys. Trends observed in global production indicate that the production

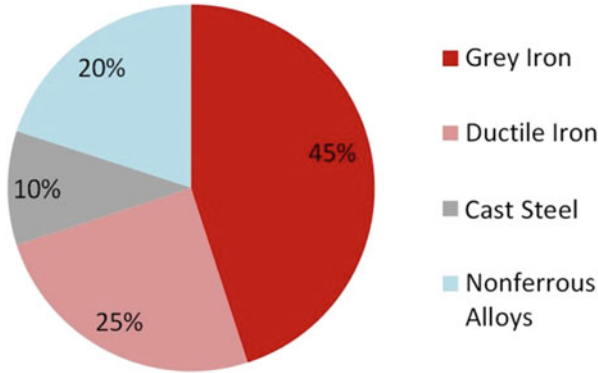


Fig. 5.54 Share of individual materials in the overall production of castings in the world (2016). (Author’s own analysis based on [12])

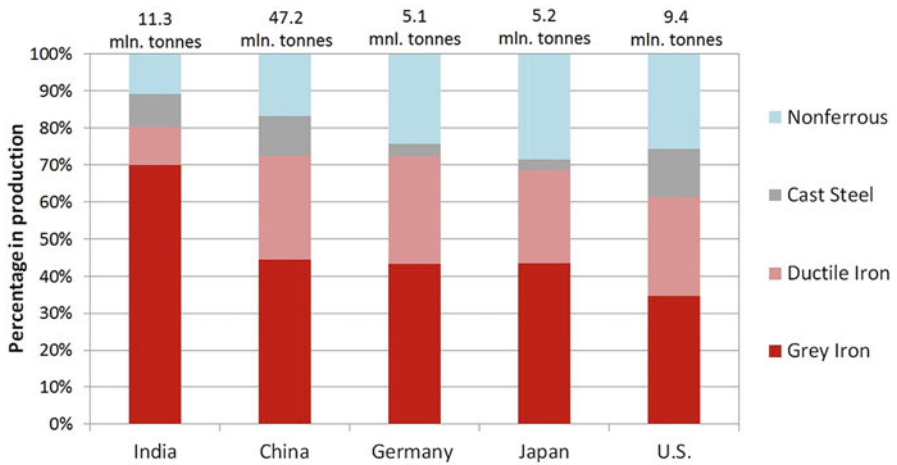


Fig. 5.55 Production of castings in top five countries producing highest amounts of cast metals (2016). (Author’s own analysis based on [12])

of ductile iron or cast iron with vermicular graphite is treated as an indicator of the development of the foundry industry in a given country and of those industries for which castings are important components of end products. This is particularly well visible in the machine and automotive industries. ADI is considered the highest achievement of cast iron technology; hence it is worth quoting several possible applications of this material (Fig. 5.55):

- Automotive: gears, connecting rods, camshafts, steering axles
- Agriculture: plough ploughshares, parts of the chassis of the agricultural machines, toothed wheels
- Mining: pump bodies and casings, rotors, crankshafts, drills

- Railway applications: locomotive wheels, clutches, suspension elements of wagons
- Arms industry: missile shells, track vehicle feet, armored vehicle casings

5.6 Summary

It is not possible to describe in a few words the vast potential of all modern types of cast iron obtained in foundry processes. Each casting method (melting process, mold material, etc.), each alloying element, and each heat and surface treatment technology will have its respective share in the properties of the final product. This is true for any group of foundry materials, and this is also true for cast iron – the most popular casting alloy in the world. Good castability, the ability to exactly reproduce even most intricate configurations and at the same time the ability to shape the structure in both micro- and nanoscale to the level that provides the highest strength properties – these are the unique features of this alloy. This chapter, showing only some isolated examples, tries to convey this simple message that modern technologies, even if based on most common metal alloys, are still capable of providing the necessary properties to modern engineering constructions. Many other possibilities of shaping cast iron properties have not been mentioned here, e.g., creating unique properties by surface layer technologies, electromagnetic processing, or creating discontinuous structures with multidimensional geometry through new casting techniques or 3D printing methods [71]. The author, however, is convinced that these are areas of future development also for high-strength casting iron alloys. One can learn about the latest achievements in scientific conferences where subject matter is focused on cast iron and other important iron alloys. These are events like the International Symposium on the Science and Processing of Cast Iron and the International Conference on Modern Steels and Iron Alloys.

References

1. World Foundry Organization, 40th census of world casting production —2005. <http://www.thewfo.com/census> Accessed 30 Sept 2019 (2006)
2. World Foundry Organization, 41st census of world casting production —2006. <http://www.thewfo.com/census> Accessed 30 Sept 2019 (2007)
3. World Foundry Organization, 42nd census of world casting production —2007. <http://www.thewfo.com/census> Accessed 30 Sept 2019 (2008)
4. World Foundry Organization, 43rd census of world casting production —2008. <http://www.thewfo.com/census> Accessed 30 Sept 2019 (2009)
5. World Foundry Organization, 44th census of world casting production. <http://www.thewfo.com/census> Accessed 30 Sept 2019 (2010)
6. World Foundry Organization, 45th census of world casting production. <http://www.thewfo.com/census> Accessed 30 Sept 2019 (2011)
7. World Foundry Organization, 46th census of world casting production. <http://www.thewfo.com/census> Accessed 30 Sept 2019 (2012)

8. World Foundry Organization, 47th census of world casting production. Dividing up the Global Market. <http://www.thewfo.com/census> Accessed 30 Sept 2019 (2014)
9. World Foundry Organization, 49th census of world casting production. Modest Growth in Worldwide Casting Market. <http://www.thewfo.com/census> Accessed 30 Sept 2019 (2015)
10. World Foundry Organization, 50th census of world casting production. Global Casting Production Stagnant. <http://www.thewfo.com/census> Accessed 30 Sept 2019 (2016)
11. World Foundry Organization, 51st census of world casting production. Global Casting Production Growth Stalls. <http://www.thewfo.com/census> Accessed 30 Sept 2019 (2017)
12. World Foundry Organization, 52nd census of world casting production. Global Casting Production Expands. <https://www.moderncasting.com/issues/december-2019> Accessed 30 Dec 2019 (2018)
13. J.J.Sobczak, E.Balcer, A.Kryczek, Polish foundry on the background of world casting. Current status and trends, Nationwide Day of the Foundryman, (Krakow 2015)
14. Podrzucki Cz. *Cast iron – structure, properties, application* (ZG STOP, Kraków, 1991)
15. Podrzucki Cz, Problems of production of castings from spheroidal cast iron ADI. Foundry J. Polish Foundrymen Assoc **10**, 260–265 (1996)
16. E. Guzik, *Processes for Refining Cast Iron - Selected Issues* (Archives of Foundry Engineering, Katowice, 2001)
17. Ductile Iron Society, Section IV. Austempered ductile iron. <https://www.ductile.org/didata/Section4/4intro.htm>. (1998) Accessed 30 Sept 2019
18. E. Fraś, *Crystallization of Metals and Alloys* (PWN, Warszawa, 1992)
19. H.K.D.H. Bhadeshia, *Bainite in Steels* (The Institute of Materials, Cambridge, 2001)
20. S. Pietrowski, Effects of Ni, Mo and Cu on the transformation of austenite into softwoods in raw castings of nodular iron. Przegląd Odlewnictwa **5**, 157–161 (1987)
21. Pietrowski St.: „Conversion of austenite - bainite, martensite in nodular cast iron”, Inżynieria Materiałowa, 1990, nr5, 115–120
22. Rivera G., Boeri R., Sikora J., Influence of the inoculation process, the chemical composition and the cooling rate, on the solidification macro and microstructure of ductile iron, Seventh International Symposium SPC17', (Barcelona 2002), Pre Pints
23. K. Sękowski, Heterogeneity of the chemical composition of the metal matrix of nodular cast iron. Foundry J. Polish Foundrymen Assoc **8-9**, 250–255 (1973)
24. J. Campbell, *Complete Casting Handbook. Metal Casting Processes, Metallurgy, Techniques and Design* (Elsevier, Butterworth-Heinemann, 2015)
25. S.I. Karsay, *Ductile iron I. Production* (QIT - Fer et Titane Inc, Quebec, 1992)
26. G. Rivera, R. Boeri, J. Sikora, Influence of the solidification microstructure on the mechanical properties of ductile iron. Int. J. Cast Metals Res. **11**, 533–538 (1999)
27. H. Bayati, R. Elliot, Influence of austenitising temperature on austempering kinetics in high Mn alloyed ductile cast iron. Mat. Sci. Technol. **11**(4), 776–786 (1995)
28. T. Kobayashi, H. Yamamoto, Development of high toughness in austempered type ductile cast iron and evaluation of its properties. Metall. Trans. A. **19A**, 319–327 (1988)
29. H. Bayati, R. Elliot, The concept of an austempered heat treatment processing window. Int. J. Cast Metals Res. **11**, 413–417 (1999)
30. L. Shen-Chin, H. Cheng-Hsun, C. Chao-Chia, F. Hui-Ping, Influence of casting size and graphite nodule refinement on fracture toughness of austempered ductile iron. Metall. Met. Trans. **29A**(10), 2511–2521 (1998)
31. E. Fraś, K. Wiencek, M. Górny, H.F. López, E. Olejnik, Grain count in castings: Theoretical background and experimental verification. Int. J. Cast Metals Res. **27**, 15–25 (2014)
32. S. Pietrowski, Ductile cast iron with a bainitic ferrite structure with austenite or bainitic ferrite. Archiwum Nauki o Materiałach **18**(4), 253–273 (1995)
33. P. Nawrocki, A. Kochański, D. Myszka, Statistical assessment of the impact of elevated contents of Cu and Ni on the properties of Austempered ductile Iron. Arch. Metall. Mater. **61**, 2147–2150 (2016)
34. P. Nawrocki, K. Wasiluk, K. Łukasik, D. Myszka, Influence of pre-heat treatment on mechanical properties of Austempered ductile cast Iron. Arch Foundry Eng **18**, 176–180 (2018)

35. T. Szykowny, T. Giętka, The hardening and tempering of hot rolling of ductile cast iron. *Arch Foundry Eng* **6**(19), 349–354 (2006)
36. European Standard Grades according to EN 1564
37. US Standard Grades according to ASTM A897/A897M-03
38. L. Jincheng, R. Elliot, The influence of cast structure on the austempering of ductile iron. Part 3. The role of nodule count on the kinetics, microstructure and mechanical properties of austempered Mn alloyed ductile iron. *Int. J. Cast Metals Res.* **12**, 189–195 (1999)
39. J.M. Schissler, J. Saverna, The effect of segregation on the formation of ADI. *J. Heat Treat.* **4**, 167–176 (1985)
40. Volgt L, Austempered ductile iron – Process control and quality assurance. Proceedings 1st International Conference on ADI, University of Michigan, Ann Arbor, USA (1986)
41. N. Darwish, R. Elliot, Austempering of low manganese ductile irons. Part 1. Processing window. *Mat. Sci. Technol.* **9**(7), 572–586 (1993)
42. N. Varahraam, O. Yanagisawa, Properties of austempered ductile iron produced in equipment designed for consecutive in-stream treatment, gravity-die casting, and direct austempering. *Cast Metal* **3**(3), 129–139 (1990)
43. S.M. Yoo, K. Moeinipour, A. Ludwig, P.R. Sahn, Numerical simulation and experimental results of in situ heat treatment austempered ductile iron. *Int. J. Cast Metals Res.* **11**, 483–488 (1999)
44. H. Bayati, R. Elliot, Influence of austenitising temperature on austempering kinetics in high Mn alloyed ductile cast iron. *Mat. Sci. Technol.* **11**(4), 776–786 (1995)
45. G. Cinceros, L. Perez, C. Campos, C. Valdes, The role of Cu, Mo and Ni on the kinetics of the bainitic reaction during the austempering of ductile irons. *Int. J. Cast Metals Res.* **11**, 425–430 (1999)
46. D.M. Moore, T.N. Rouns, K.B. Rundman, The relationship between microstructure and tensile properties in ADI. *Am. Foundry Soc.* **95**, 765–774 (1987)
47. A. Trudel, E. Gangne, Effect of composition and heat treatment parameters on the characteristics of austempered ductile iron. *Can. Metall. Q.* **36**(5), 289–298 (1997)
48. S. Dymski, *Kształtowanie struktury i właściwości mechanicznych żeliwa sferoidalnego podczas izotermicznej przemiany bainitycznej* (Wyd. Uczelniane ATR, Bydgoszcz, 1999)
49. J. Aranzabal, I. Guiterrez, J.M. Rodriguez-Ibabe, J.J. Urcola, Influence of the amount and morphology of retained austenite on the mechanical properties of an austempered ductile iron. *Metall. Mater. Trans. A* **28A**, 1143–1156 (1997)
50. D. Srinivasmurthy, P. Prasad Rao, Formation of strain-induced martensite in austempered ductile iron. *J. Mater. Sci.* **43**, 357–367 (2008)
51. J.L. Garin, R.L. Mannheim, Strain-induced martensite in ADI alloys. *J. Mater. Process. Technol.* **143–144**, 347–351 (2003)
52. D. Myszka, Austenite-martensite transformation in austempered ductile iron. *Arch. Metall. Mater.* **52**, 475–480 (2007)
53. D.J. Moore, J.R. Parolini, K.B. Rundman, On the kinetics of austempered gray cast iron. *AFS Trans.* **111**, 911–930 (1990)
54. J. Yang, S.K. Putatunda, Influence of a novel two-step austempering process on the strain-hardening behaviour of austempered ductile cast iron (ADI). *Mater. Sci. Eng. A* **382**, 265–279 (2004)
55. J. Yang, S.K. Putatunda, Effect of microstructure on abrasion wear behavior of austempered ductile cast iron (ADI) processed by a novel two-step austempering process. *Mater. Sci. Eng. A* **406**, 217–228 (2005)
56. D. Myszka, K. Wasiluk, E. Skołek, W. Świątnicki, Nanoausferritic matrix of ductile iron. *Mater. Sci. Technol.* **31**, 829–834 (2015)
57. M. Pachowski, Hartowanie bainityczne żeliwa sferoidalnego. *Metaloznawstwo i Obróbka Ciepła* **43**, 16–19 (1980)
58. K. Moeinipour, P.R. Sahn, ADI - Kokillengießverfahren mit gekoppelter in-situ-Wärmebehandlung. *Giessereiforschung* **54**(1), 22–28 (2002)

59. J. Sikora, R. Boeri, Solid state transformations in ductile iron – influence of prior austenite matrix microstructure. *Int. J. Cast Metals Res.* **11**, 395–400 (1999)
60. J. Massone, R. Boeri, J. Sikora, Production of ADI by hot shake out – Microstructure and mechanical properties. *Int. J. Cast Metals Res.* **11**, 419–424 (1999)
61. Rivera G, Boeri R, Sikora J, Influence of the inoculation process, the chemical composition and the cooling rate, on the solidification macro and microstructure of ductile iron. Pre prints of Seventh International Symposium SPC17', Barcelona, Spain (2002)
62. J. Tybulczuk, D. Myszka, A. Pytel, A. Kowalski, M. Kaczorowski, Structural and mechanical investigations of ductile iron directly austempered from the casting mould. *Arch. Foundry Eng.* **2**(4), 460 (2002)
63. D. Myszka, M. Kaczorowski, Direct austempering of ductile iron produces in sand moulds. *Acta Metalurgica Slovaca* **3**, 271–276 (2001)
64. Nofal AA The current status of the metallurgy and processing of austempered ductile iron (ADI). Proceedings of 10th international symposium on the science and processing of cast Iron – SPCI10, Cairo, Egypt (2010)
65. M. Soliman, H. Palkowski, Nofal, Multiphase ausformed austempered ductile iron. *Arch. Metall. Mater.* **62**(3), 1493–1498 (2017)
66. B.N. Olson, D.J. Moore, K.B. Rundman, G.R. Simula, Potential for practical applications of ausforming austempered ductile iron. *AFS Trans.* **112**, 845–850 (2003)
67. D. Myszka, L. Cybula, A. Wiczorek, Influence of heat treatment conditions on microstructure and mechanical properties of austempered ductile iron after dynamic deformation test. *Arch. Metall. Mater.* **59**, 1181–1189 (2014)
68. A.N. Wiczorek, Operation-oriented studies on wear properties of surface-hardened alloy cast steels used in mining in the conditions of the combined action of dynamic forces and an abrasive material. *Arch. Metall. Mater.* **62**(1), 119–128 (2017)
69. A. Wiczorek, D. Myszka, Abrasive wear properties of Fe-based alloys designed for mining applications. *Arch. Metall. Mater.* **62**(3), 1521–1534 (2017)
70. K.L. Hayrynen, K.R. Brandenburg, *Carbidic Austempered Ductile Iron (CADI) – The New Wear Material* (Applied Process Technologies Division, Livonia, 2003)
71. H. Fayazfara, M. Salariana, A. Rogalskya, D. Sarkera, P. Russoa, V. Paserinb, E. Toyserkani, A critical review of powder-based additive manufacturing of ferrous alloys: Process parameters, microstructure and mechanical properties. *Mater. Des.* **144**, 98–128 (2018)